

Multifactor Quadratic Hobson and Rogers models

Paolo Foschi*

A multi-factor extension of the Hobson and Rogers (HR) model, incorporating a quadratic variance function (QHR model), is proposed and analysed. The QHR model allows for greater flexibility in defining the moving average filter while maintaining the Markovian property of the original HR model. The use of a quadratic variance function permits the characterisation of weak-stationarity conditions for the variance process and allows for explicit expressions for forward variance. Under the assumption of stationarity, both the variance and the squared increment processes exhibit an ARMA autocorrelation structure. The stationary distribution of the prototypical scalar QHR model is that of a translated and rescaled Pearson type IV random variable. A numerical exercise illustrates the qualitative properties of the QHR model, including the implied volatility surface and the term structures of forward variance, at-the-money (ATM) volatility, and ATM skew.

Keywords: Hobson and Rogers Model, Path Dependent Volatility, Stochastic Volatility, Polynomial Models, Stationarity, Term Structure of Variance, VIX

MSC: 60H10, 60G10, 91G20, 91G30

1. Introduction

In recent years there has been a growing interest in path dependent volatility (PDV) continuous time models, primarily driven by the need of pricing VIX derivatives [13, 16]. The Hobson and Rogers (HR) model was one of the first models in that class [19]. In the HR model the volatility is a deterministic function of the offset of the current log-price level $x_t = \log(S_t)$ with respect to its exponential moving average. More precisely, the HR offset is defined as

$$y_t = x_t - \int_{-\infty}^t \varphi(t-s)x_s ds, \quad \varphi(t) = \lambda e^{-\lambda t},$$

*Dept. of Statistical Sciences, University of Bologna (paolo.foschi2@unibo.it).

where $\lambda > 0$, and the risk-neutral dynamics of x_t is

$$x_t = -\frac{1}{2}\sigma_t^2 dt + \sigma_t dW_t \quad (1)$$

where $\sigma_t^2 = f(y_t)$ for some function $f : \mathbb{R} \rightarrow \mathbb{R}_+$ that links the offset to the underlying spot variance. One of the best features of the HR approach is that the dynamics of x_t and y_t is Markovian. Indeed, the offset process solves the stochastic differential equation (SDE)

$$dy_t = -\lambda y_t dt + dx_t. \quad (2)$$

Still, that approach leaves some freedom to the practitioner by allowing the choice of the memory parameter λ and of the function f that links the offset level to the instantaneous variance. The performances of that approach have been tested by Foschi and Pascucci [12].

Another advantage in using the HR model is the fact that the model dynamics, and in turn, the resulting pricing functions, are “non-dimensional” [20]. Indeed, the SDEs (1) and (2) are autonomous, since their coefficients do not depend on the time variable, and the link function only depends on the offset y_t . Being the difference of a log-price and an average of log-prices, y_t is a non-dimensional quantity (analogous to a log-ratio).

The downside of the HR models is the excessive rigidity in the choice of moving average filter φ . A tentative generalisation in that direction is represented by the so called Path Dependent Volatility model (PDV). In that model, a different filter function can be chosen, but at the cost of obtaining SDEs that are not autonomous, i.e. their coefficients depend on absolute time [11, 18]. As a consequence, PDV model parameters tend to be heavily time- and contingency-dependent.

The purpose of this work is to generalise the HR model to a parametric model which allows more freedom in the choice of the moving average filter without losing the advantages autonomous SDEs and a non-dimensional volatility specification. A second modelling objective is to obtain explicit expressions of the conditional expectations of the first two moments of the variance process.

These results allow to obtain the autocorrelation structure of the variance process allowing to characterise the weak-stationarity of the spot variance process. With respect to those issues, notice that, the principal component analysis, which is often used in finance to present stylised facts and justify term structure models, requires weak-stationarity [26]. Moreover, mean reversion and stationarity represent major selling points in the marketing of variance related products like VIX¹.

Under the assumptions of weak-stationarity, the variance process and the squared increments have the autocovariance structure of an ARMA process [4]. But, differently from [2] or [3], that structure is here obtained without introducing additional Brownian motions and remaining in a diffusive setup.

As an additional advantage, the model considered here allows for an explicit formula of the conditional variance. In other words, the term structure of forward variance can

¹See CBOE’s VIX page https://www.cboe.com/tradable_products/vix/.

be explicitly computed without the need of a Monte Carlo integration, simplifying model calibration tasks.

Here, the HR offset y_t is generalised to a p -dimensional process having dynamics

$$dy_t = -\mathbf{A}y_t dt + \mathbf{b}\sigma_t dW_t \quad (3)$$

where $\mathbf{b} \in \mathbb{R}^p$, all the eigenvalues of $\mathbf{A} \in \mathbb{R}^{p \times p}$ have positive real part. That process corresponds to exponential moving average:

$$\mathbf{y}_t = \int_{-\infty}^t \mathbf{A}e^{-\mathbf{A}(t-s)} \mathbf{b}(\xi_t - \xi_s) ds,$$

where ξ_t is the process with dynamics $d\xi_t = \sigma_t dW_t = dS_t/S_t$. Note that, in (2) the offset process was averaging the log-price innovations dx_t , while in (3) the average is performed only on their unpredictable part $\sigma_t dW_t = dS_t/S_t$. Next the offsets in \mathbf{y}_t can be linearly combined to obtain an offset process $\tilde{y}_t = \mathbf{w}^T \mathbf{y}_t$, $\mathbf{w} \in \mathbb{R}_+^p$. When $\mathbf{b}^T \mathbf{w} = 1$, that choice corresponds to an offset computed w.r.t. a moving average with a filter that depends on \mathbf{A} , \mathbf{b} and \mathbf{w} :

$$\tilde{y}_t = \xi_t - \int_{-\infty}^t \varphi(t-s) \xi_s ds, \quad \varphi(t) = \mathbf{w}^T \mathbf{A}e^{-\mathbf{A}t} \mathbf{b}. \quad (4)$$

Note that $\varphi(t)$ is an exponential polynomial: $\varphi(t) = \sum_i t^{n_i} e^{\alpha_i - \beta_i t}$ for some finite set of coefficients $\{\alpha_i, \beta_i \in \mathbb{C}\}$.

The second element of the HR modelling consists in the specification of the variance link function. In order to contain the number of parameter and to obtain a analytically tractable model the spot variance is defined as a quadratic function of \mathbf{y}_t :

$$\sigma_t^2 = \alpha + 2\boldsymbol{\beta}^T \mathbf{y}_t + \mathbf{y}_t^T \boldsymbol{\Gamma} \mathbf{y}_t, \quad (5)$$

where $\alpha > 0$, $\boldsymbol{\Gamma} \in \mathbb{R}^{p \times p}$ and $\boldsymbol{\beta} \in \mathbb{R}^p$ is such that $\sigma_t^2 > 0$ for all $\mathbf{y}_t \in \mathbb{R}^p$. It will be shown that, with this choice of the variance link, the variance mean-reversion, its conditional expectation and weak-stationarity can be explicitly characterised.

Again, when $\boldsymbol{\beta} = \beta_0 \mathbf{w}$ and $\boldsymbol{\Gamma} = \gamma_0 \mathbf{w} \mathbf{w}^T$, the spot variance is a quadratic function \tilde{y}_t . Thus, the model given by (3) and (5), encompass HR models where the moving average filter is generalised to an exponential polynomial.

Models based on exponential polynomial filters have been considered in [1, 5, 15, 17]. In particular, multifactor diffusion models have been used to approximate Rough Volatility models [15, 17]. The Quadratic Rough Heston model is analogous the one here proposed in using a quadratic function to link a path moving average to the instantaneous variance coefficient [13]. For a review on rough and non-rough volatility models see [9]. Note that the actual roughness of financial volatility processes is not a settled question [7]. Also, discrete time models where the volatility depends on different filters (different scales), have been around for some time. For a couple of different successful approaches, see the Component GARCH and the Realised Volatility models [6, 8].

The paper is structured as follows. In section 2, the model is presented with some results on its solution. Identification of the model is briefly discussed in subsection 2.1. Then, in subsection 2.2, homogeneity properties of the transition density and pricing functions are discussed. Next, subsection 2.3 characterises the model as a path-dependent volatility one where the latent factor consists on auto-regressive (exponential) filters. Then, in subsection 2.4, conditional moments of the offset and variance processes are characterised in terms of matrix exponentials. That characterisation allows to obtain sufficient condition for the mean reversion or weak-stationarity of the variance and conditional variance processes (subsection 2.5). A simple algorithm for computing the shape of the principal component decomposition of the forward variance term structure is presented in subsection 2.6.

In section 3, a couple of special cases are presented with an extensive set of numerical examples showing the characteristics and potential flexibility of this class of models. The first model considered is the scalar (classical) QHR model. Given its simplicity, that model allows for weak-stationarity conditions to be explicitly defined. Moreover, it is shown that under those conditions there exists a stationary solution for the offset-process y_t . Moreover, the stationary distribution for y_t consists on a Pearson type IV distribution [22], that reduces to a scaled student-t distribution for the symmetric case $\beta = 0$. The second class of models presented in Section 3 are the rank-one models. In this class of models, the instantaneous variance is function of a single offset process obtained as in (4). In that case, we could not simplify further the result obtained in section 2 and their analysis only consists on a numerical one.

An additional section, Appendix A, contains the proofs of the results reported in the previous sections.

1.1. Notation

Most of the notational conventions used in the rest of this work are here introduced. The set of n -dimensional real vectors and $m \times n$ real matrices are denoted by \mathbb{R}^n and $\mathbb{R}^{m \times n}$, respectively. Vectors are represented using lowercase bold symbols and matrices by means of bold capital characters. Vectors are always meant to be column vectors, that is an n -vector is a $n \times 1$ matrix. The transpose of a matrix \mathbf{A} is denoted by \mathbf{A}^T . The identity matrix and its i -th column are denoted by \mathbf{I} and \mathbf{e}_i , respectively. Their dimensions should be deduced from the context. If necessary the $n \times n$ identity will be denoted by \mathbf{I}_n . The determinant and the trace operators are denoted by $\text{tr}(\mathbf{A})$ and $\det(\mathbf{A})$, respectively. If not explicitly specified, vector norms are 2-norms: $\|\mathbf{x}\| = \|\mathbf{x}\|_2 = (\mathbf{x}^T \mathbf{x})^{\frac{1}{2}}$ for $\mathbf{x} \in \mathbb{R}^n$, and matrix norms are induced 2-norms: $\|\mathbf{A}\| = \max_{\mathbf{x}} \|\mathbf{A}\mathbf{x}\|_2 / \|\mathbf{x}\|_2$. The expectation of a vector (matrix) consists on the vector (matrix) of the expectations.

The sets of real $m \times n$ -dimensional matrices with non-negative elements is denoted by $\mathbb{R}_+^{m \times n}$ and that of $n \times n$ real, symmetric and positive semi-definite matrices by \mathcal{S}_+^n . Let $\mathbf{A} \in \mathbb{R}^{m \times n}$, $\mathbf{A} \geq 0$ means that $\mathbf{A} \in \mathbb{R}_+^{m \times n}$ (element-wise). Analogously, $\mathbf{A} \geq \mathbf{B}$ if and only if $\mathbf{A} - \mathbf{B} \geq 0$.

If $\mathbf{A} \in \mathbb{R}^{m \times n}$, $\text{Vec}(\mathbf{A}) \in \mathbb{R}^{mn}$ is the vector obtained by stacking the columns of \mathbf{A} . The Kronecker product of $\mathbf{A} \in \mathbb{R}^{m \times n}$ and $\mathbf{B} \in \mathbb{R}^{p \times q}$ is represented by $\mathbf{A} \otimes \mathbf{B}$ and has

dimensions $mp \times nq$. Moreover, $\mathbf{A}^{\otimes 0} = 1$ and $\mathbf{A}^{\otimes k} = \mathbf{A} \otimes \mathbf{A}^{\otimes(k-1)}$ for $k \geq 1$ and $\mathbf{A} \in \mathbb{R}^{m \times n}$. The definitions of the Vec and Kronecker product operators and a review of their properties can be found in [21].

2. The QHR Model

The QHR model is specified as follows. The (risk-neutral) dynamics of the discounted log-price x_t of the latent vector \mathbf{y}_t is given by

$$dx_t = -\frac{1}{2}\sigma_t^2 dt + \sigma_t dW_t, \quad (6a)$$

$$d\mathbf{y}_t = -\mathbf{A}\mathbf{y}_t dt + \mathbf{b}\sigma_t dW_t, \quad (6b)$$

$$\sigma_t^2 = \alpha + 2\mathbf{y}_t^T \boldsymbol{\beta} + \mathbf{y}_t^T \boldsymbol{\Gamma} \mathbf{y}_t, \quad (6c)$$

where W_t is a standard Brownian motion on a filtration $(\mathcal{F}_t)_{t \geq 0}$ of a probability space $(\Omega, \mathcal{F}, \mathbb{P})$. The parameters $\mathbf{A} \in \mathbb{R}^{p \times p}$, $\mathbf{b} \in \mathbb{R}^p$, $\alpha \in \mathbb{R}$, $\boldsymbol{\beta} \in \mathbb{R}^p$ and $\boldsymbol{\Gamma} \in \mathbb{R}^{p \times p}$ satisfy the following assumption which is sufficient to guarantee that the SDEs (6a) and (6b) has a unique non-exploding solution in finite time (see Lemma 1 below).

Assumption 1 *The eigenvalues of \mathbf{A} are real and positive, $\alpha > 0$, $\begin{pmatrix} \alpha & \boldsymbol{\beta}^T \\ \boldsymbol{\beta} & \boldsymbol{\Gamma} \end{pmatrix}$ is positive semidefinite and (x_0, \mathbf{y}_0) is \mathcal{F} -measurable with $\mathbb{E}[x_0^2 + \|\mathbf{y}_0\|^4] < \infty$.*

Lemma 1 *Under Assumption 1 the SDE (6) has a unique non-exploding in finite time solution.*

PROOF The proof consists on exploiting the standard hypothesis of a system of SDEs. While the coefficients of the system of SDEs (6a) and (6b) do not satisfy the standard hypothesis, adding to that system the dynamics of $\mathbf{q}_t = \mathbf{y}_t \otimes \mathbf{y}_t$ results in a system of SDEs whose coefficients are Lipschitz continuous and linearly bounded.

Indeed,

$$d\mathbf{q}_t = (\bar{\mathbf{b}}\sigma_t^2 - \bar{\mathbf{A}}\mathbf{q}_t)dt + (\mathbf{b} \otimes \mathbf{y}_t + \mathbf{y}_t \otimes \mathbf{b})\sigma_t dW_t, \quad \text{and} \quad \sigma_t^2 = \alpha + 2\mathbf{y}_t^T \boldsymbol{\beta} + \boldsymbol{\gamma}^T \mathbf{q}_t \quad (7)$$

where $\bar{\mathbf{b}} = \mathbf{b} \otimes \mathbf{b}$, $\bar{\mathbf{A}} = \mathbf{A} \otimes \mathbf{I}_p + \mathbf{I}_p \otimes \mathbf{A}$ and $\boldsymbol{\gamma} = \text{Vec}(\boldsymbol{\Gamma})$. Thus, since σ_t^2 is an affine function of the state process $(x_t; \mathbf{y}_t; \mathbf{q}_t)$, the trend coefficients of the system (6) and (7) are affine functions of the state processes. Moreover, the diffusion coefficients of x_t , \mathbf{y}_t and \mathbf{q}_t are, respectively, given by σ_t , $\mathbf{b}\sigma_t$ and $(\mathbf{b} \otimes \mathbf{y}_t + \mathbf{y}_t \otimes \mathbf{b})\sigma_t$. Since $\alpha > 0$ by Assumption 1, the σ_t and, in turn, $\mathbf{b}\sigma_t$, are Lipschitz function of \mathbf{y}_t . Regarding the diffusion coefficient of \mathbf{q}_t , its squared norm is given by

$$\begin{aligned} \|(\mathbf{b} \otimes \mathbf{y}_t + \mathbf{y}_t \otimes \mathbf{b})\|^2 \sigma_t^2 &= 2\left(\mathbf{b}^T \mathbf{b} \mathbf{y}_t^T \mathbf{y}_t + (\mathbf{b}^T \mathbf{y}_t)^2\right) \sigma_t^2 \\ &\leq (A_1 + A_2 \|\mathbf{q}_t\|) \sigma_t^2 \leq (B_1 + B_2 \|\mathbf{q}_t\|^2), \end{aligned}$$

for some positive constants A_1, A_2, B_1 and B_2 . It follows that this diffusion coefficient is Lipschitz with at most linear growth. Consider also the assumption Assumption 1.c, the

system of SDEs (6) and (7) satisfies the standard hypothesis and thus it has a unique non-exploding in finite time solution. By construction, the system of SDEs (6) and (7), with initial condition $\mathbf{q}_0 = \mathbf{y}_0 \otimes \mathbf{y}_0$, coincides with the system (6). It follows that also the latter has a unique non-exploding in finite time solution. \blacksquare

Here, the dynamics (6) has not been deliberately placed under the real or the risk-neutral measure. The QHR model can be used either for modelling the actual price trajectories or for pricing purpose. That distinction will be made also in the rest of the paper: there will not be tilde-W Brownian motion. Conditional and forward instantaneous variances will be the mathematical object. Nevertheless, it is interesting to investigate conditions where the same class of QHR models can be used for both the real and the risk-neutral measures. The following remark present one such condition.

Remark 1 (A change of measure that preserves the model structure) Let $W_t = \tilde{W}_t + \int_0^t \frac{\mu_0 + \mu_1^T \mathbf{y}_s}{\sigma_s} ds$ for some fixed $\mu_0 \in \mathbb{R}$ and $\mu_1 \in \mathbb{R}^p$ such that $\mu_1^T \Lambda^{-1} \mathbf{b} \neq 1$. Assuming that \tilde{W}_t is a Brownian motion under a measure \tilde{P} equivalent to P , the measure associated to the Brownian motion W_t . Then, x_t and \mathbf{y}_t have dynamics

$$dx_t = (\mu_0 + \mu_1^T \mathbf{y}_t - \frac{1}{2} \sigma_t^2) dt + \sigma_t d\tilde{W}_t, \quad (8a)$$

$$d\mathbf{y}_t = \mu_0 \mathbf{b} - (\Lambda - \mathbf{b} \mu_1^T) \mathbf{y}_t dt + \mathbf{b} \sigma_t d\tilde{W}_t. \quad (8b)$$

Now, let $\tilde{\Lambda} = \Lambda - \mathbf{b} \mu_1^T$ and $\tilde{\mathbf{y}}_t = \mathbf{y}_t - \mu_0 \tilde{\Lambda}^{-1} \mathbf{b}$. That definition is well posed because $\mu_1^T \Lambda^{-1} \mathbf{b} \neq 1$ implies that $\tilde{\Lambda}$ is non-singular. It follows that,

$$d\tilde{\mathbf{y}}_t = -\tilde{\Lambda} \tilde{\mathbf{y}}_t dt + \mathbf{b} \sigma_t dW_t,$$

and that σ_t^2 is a quadratic function of \mathbf{y}_t . That is, the volatility process σ_t (but not the underlying) follows a QHR model under the real world measure \tilde{P} . However, notice that, without specifying additional assumptions, $\tilde{\Lambda}$ may have complex eigenvalues or negative eigenvalues. That is, the first condition of assumption Assumption 1 may not be satisfied.

The interpretation is the following, in the real world measure, S_t can have a stochastic trend μ_t which is an affine function of the offset vector \mathbf{y}_t : $dS_t = \mu_t S_t dt + \sigma_t S_t dW_t$. $\mu_t = \tilde{\mu}_0 + \tilde{\mu}_1^T \tilde{\mathbf{y}}_t$ with $\tilde{\mu}_0 \in \mathbb{R}$ and $\tilde{\mu}_1 \in \mathbb{R}^p$ fixed. \blacksquare

2.1. Identification

Let $\tilde{\mathbf{y}}_t = \mathbf{M}^{-1} \mathbf{y}_t$ for some non-singular matrix $\mathbf{M} \in \mathbb{R}^{p \times p}$. Then, (6b) and (6c) can be rewritten as

$$d\tilde{\mathbf{y}}_t = -\tilde{\Lambda} \tilde{\mathbf{y}}_t dt + \tilde{\mathbf{b}} \sigma_t dW_t, \quad \sigma_t^2 = \alpha + 2\tilde{\mathbf{y}}_t^T \tilde{\boldsymbol{\beta}} + \tilde{\mathbf{y}}_t^T \tilde{\boldsymbol{\Gamma}} \tilde{\mathbf{y}}_t,$$

where $\tilde{\Lambda} = \mathbf{M}^{-1} \Lambda \mathbf{M}$, $\tilde{\mathbf{b}} = \mathbf{M}^{-1} \mathbf{b}$, $\tilde{\boldsymbol{\beta}} = \mathbf{M}^T \boldsymbol{\beta}$ and $\tilde{\boldsymbol{\Gamma}} = \mathbf{M}^T \boldsymbol{\Gamma} \mathbf{M}$. That is, a change of basis on the space of the latent process \mathbf{y}_t results in a model having the same specification of (6). In other words, model (6) is not identified w.r.t. a similarity transform applied

to \mathbf{A} . To resolve that identification issue, in the following it will be assumed that \mathbf{A} has the Jordan's structure

$$\mathbf{A} = \bigoplus_{i=1}^m \lambda_i \mathbf{D}_i, \quad \mathbf{D}_i = \begin{pmatrix} 1 & 0 & 0 & \cdots & 0 \\ -1 & 1 & 0 & \ddots & \vdots \\ 0 & -1 & 1 & \ddots & 0 \\ \vdots & \ddots & \ddots & \ddots & 0 \\ 0 & \cdots & 0 & -1 & 1 \end{pmatrix} \in \mathbb{R}^{n_i \times n_i}, \quad \lambda_1 > \cdots > \lambda_m. \quad (9)$$

Notice that the assumption on distinct eigenvalues is necessary because if \mathbf{A} has two blocks having the identical eigenvalue, then, corresponding to those two blocks, \mathbf{y}_t have two sub-vectors that correspond to the same path integrals of $\sigma_t dW_t$ and, consequently, have identical values. It follows that, those two sub-vectors and their coefficients in the variance specification can be aggregated and reducing the size of the model.

Now, even under the specification (9), the model is still not identified w.r.t. the above similarity transformations when $\mathbf{M} = \bigoplus_{i=1}^m \mu_i \mathbf{I}_{n_i}$. In order make the model identified w.r.t. those transformations, the coefficient vector \mathbf{b} is assumed to be fixed and given by

$$\mathbf{b} = \text{Vec}(\{\mathbf{b}_i\}_{i=1}^m), \quad \mathbf{b}_i = \mathbf{e}_1 \in \mathbb{R}^{n_i}. \quad (10)$$

Clearly, a different set of constraints could have been chosen to obtain identification. For instance, often, for continuous ARMA models and for the COGARCH model, a companion matrix form is used [3]. The above Jordan structure has been adopted because it simplifies the characterisation of its matrix exponentials.

Resuming the following assumption will be made for the identification of the QHR model.

Assumption 2 (Identification - Jordan canonical form) *The matrix \mathbf{A} and the vector \mathbf{b} have the structure given in (9) and (10).*

2.2. Homogeneity properties

We emphasise the following properties of the dynamics given in (6a) and (6b). This system of SDEs is

- Markovian,
- autonomous (the coefficients do not depend on t) and
- free of “local volatility” mechanisms.

For the last property we mean that the trend and diffusion coefficients do not directly depend on the level of the log-price x_t .

One the main consequence of those properties is that, conditional on \mathcal{F}_t , the distribution of the log-return $x_T - x_t$, $T > t$, does not depend on x_t , but only on the offset process \mathbf{y}_t . Moreover, that distribution does not depend neither on the absolute dates t

and T . More precisely, fix an horizon $\bar{T} > 0$ and assume that the process (x_t, \mathbf{y}_t) admits a transition density from t to T , $0 \leq t < T$. Then, calling $p(T, x_T, \mathbf{y}_T; t, x_t, \mathbf{y}_t \mid \mathbf{A}, \alpha, \beta, \Gamma)$ that density can be written as

$$p(T, x_T, \mathbf{y}_T; t, x_t, \mathbf{y}_t \mid \mathbf{A}, \alpha, \beta, \Gamma) = p_0(x_T - x_t, \mathbf{y}_T; \mathbf{y}_t, T - t \mid \mathbf{A}, \alpha, \beta, \Gamma),$$

for some density $p_0(\cdot, \cdot; \mathbf{y}_t, T - t \mid \mathbf{A}, \alpha, \beta, \Gamma)$. Moreover, from (6a), (6b) and (6c) the function p_0 satisfies the time-scaling property

$$p_0(x, \mathbf{y}; \mathbf{y}_0, cT \mid \mathbf{A}, \alpha, \beta, \Gamma) = p_0(x, \mathbf{y}; \mathbf{y}_0, T \mid c\mathbf{A}, c\alpha, c\beta, c\Gamma), \quad c > 0.$$

It follows that the price of a Call option,

$$\text{Call}(S, K, \mathbf{y}, t, T) = \mathbb{E}[(e^{x_T} - K)_+ \mid x_t = \log(S), \mathbf{y}_t = \mathbf{y}],$$

is 0-homogeneous w.r.t. time and 1-homogeneous w.r.t. prices:

$$\text{Call}(S, K, \mathbf{y}, t, T) = S \text{Call}(1, K/S, \mathbf{y}; 0, T - t).$$

By the Put-Call parity, Put prices have the same homogeneity properties.

This property means that the option's relative price (Call/S) depends only on the moneyness (K/S), on the current level of the offsets (\mathbf{y}) and on the time-to-maturity ($T - t$). In other words, those relative price surface, $(K/S, T - t) \rightarrow \text{Call}/S$, depends on the offsets and not of the absolute underlying price.

For options on spot variance, as (6b) is Markovian, the price depends only on the offset levels and time-to-maturity:

$$\mathbb{E}[\varphi(\sigma_T^2) \mid \mathbf{x}_t = x, \mathbf{y}_t = \mathbf{y}] = \mathbb{E}[\varphi(\sigma_{T-t}^2) \mid \mathbf{x}_0 = 0, \mathbf{y}_0 = \mathbf{y}].$$

Analogous considerations are valid for derivatives on the integrated variance.

2.3. Moving average filters

Here, an heuristic characterisation of the latent factor \mathbf{y}_t as moving averages of the price trajectories is given. The presentation is only formal with heavy mathematical shortcuts.

Under Assumptions 1 and 2, consider the moving average process defined in (4) and distinguish the two extreme cases of distinct roots ($n_1 = n_2 = \dots = n_m = 1$) and one single root ($m = 1, n_1 = n$) and then the general case.

- Distinct roots: $m \geq 1, p = m$ ($n_1 = \dots = n_m = 1$).

In this case, \mathbf{A} is a diagonal matrix and \mathbf{b} is a vector of all ones:

$$\mathbf{A} = \text{diag}(\lambda_1, \dots, \lambda_m), \quad \mathbf{b} = \mathbf{1}.$$

Then, i -th element of \mathbf{y}_t is given by

$$y_{it} = \xi_t - \int_{-\infty}^t \lambda_i e^{-\lambda_i(t-s)} \xi_s ds.$$

That is, y_{it} is the deviation of ξ_t from its exponential moving average with parameter λ_i . The moving average filter used to compute y_{it} is the function $\varphi_i : s \in \mathbb{R}_+ \rightarrow \lambda_i e^{-\lambda_i s}$, which is strictly positive and integrates to one. Then, the application of that filter corresponds to an average.

Moreover, the elements of \mathbf{y}_t can be linearly combined to obtain another filter. For instance, if $\mathbf{w} \in \mathbb{R}_+^p$ and $\mathbf{w}^T \mathbf{b} = \mathbf{w}^T \mathbf{1} = 1$, then

$$\mathbf{w}^T \mathbf{y}_t = \xi_t - \int_{-\infty}^t \varphi(t-s) \xi_s ds, \quad \varphi(t) = \sum_{i=1}^n w_i \lambda_i e^{-\lambda_i t}.$$

Again, φ is positive and has unit integral.

- Single root with multiplicity n : $m = 1$, $n_1 = n \geq 1$, $p = n$.

In this case $\mathbf{A} = \lambda_1 \mathbf{D}$ and $\mathbf{b} = \mathbf{e}_1$. It turns out that

$$e^{-\mathbf{A}t} = e^{-\lambda t} \begin{pmatrix} 1 & 0 & 0 & \cdots & 0 \\ (\lambda t) & 1 & 0 & \ddots & \vdots \\ \frac{(\lambda t)^2}{2} & (\lambda t) & 1 & \ddots & 0 \\ \vdots & \ddots & \ddots & \ddots & 0 \\ \frac{(\lambda t)^{n-1}}{(n-1)!} & \cdots & \frac{(\lambda t)^2}{2} & (\lambda t) & 1 \end{pmatrix}$$

Then $e^{-\mathbf{A}t} \mathbf{b}$ and, in turn, $\mathbf{A} e^{-\mathbf{A}t} \mathbf{b}$ are, respectively, given by

$$e^{-\mathbf{A}t} \mathbf{b} = e^{-\lambda t} \begin{pmatrix} 1 \\ (\lambda t) \\ \frac{(\lambda t)^2}{2} \\ \vdots \\ \frac{(\lambda t)^{n-1}}{(n-1)!} \end{pmatrix} \quad \text{and} \quad \mathbf{A} e^{-\mathbf{A}t} \mathbf{b} = \lambda e^{-\lambda t} \begin{pmatrix} 1 \\ \lambda t - 1 \\ \frac{(\lambda t)^2}{2} - \lambda t \\ \vdots \\ \frac{(\lambda t)^{n-1}}{(n-1)!} - \frac{(\lambda t)^{n-2}}{(n-2)!} \end{pmatrix}.$$

The first element of \mathbf{y}_t is given by the offset

$$y_{1t} = \xi_t - \int_{-\infty}^t \psi_1(t-s) \xi_s ds, \tag{11a}$$

and the remaining ones by the offsets

$$y_{it} = \int_{-\infty}^t \psi_i(t-s) \xi_s ds - \int_{-\infty}^t \psi_{i-1}(t-s) \xi_s ds, \quad i > 1. \tag{11b}$$

where $\psi_i(t) = \lambda e^{-\lambda t} \frac{(\lambda t)^{i-1}}{(i-1)!}$, $1 \leq i \leq n$. Since $\lambda > 0$, $\int_0^\infty \psi_i(t) dt = 1$ for all i . It turns out that the filter φ defined in (4) can be written as

$$\varphi(t) = \sum_{i=1}^{n-1} (w_i - w_{i+1}) \psi_i(t) + w_n \psi_n(t).$$

Then, if $w_1 = 1$ and $w_i \geq w_{i+1} \geq 0$, $i < n$, the function φ is positive and integrates to one. Figure 1 shows the functions φ_i , $i = 1, \dots, 5$ when $\lambda = 4$ and one example of $\psi(t)$ when $\mathbf{w} = (1; 0.8; 0.6; 0.4)$. Note that, while the filter ψ_1 corresponds to an exponential moving average, ψ_2, ψ_3 and ψ_4 correspond to moving averages that concentrate more weight near a lag of 0.25, 0.5 and 0.75 years. The processes y_{2t} , y_{3t} and y_{4t} are offsets between those moving average. Moreover, φ is an average of the four filters ψ_1, \dots, ψ_4 : $\varphi = 0.2\psi_1 + 0.2\psi_2 + 0.2\psi_3 + 0.4\psi_4$.

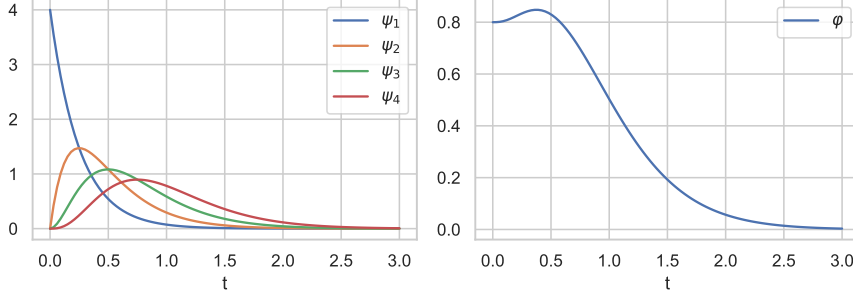


Figure 1: Left plot: the filters $\psi_1(t), \dots, \psi_4(t)$ when $\lambda = 4$. Right plot: the moving average filter $\varphi(t)$ when $\lambda = 4$ and $\mathbf{w}^T = (1 \ 0.8 \ 0.6 \ 0.4)$.

- $m > 1$, $n_i \geq 1$, $i = 1, \dots, m$.

In this case \mathbf{A} is a block diagonal matrix with the i -th block being $\lambda_i \mathbf{D}$. Moreover, \mathbf{b} is a vector with blocks given by \mathbf{e}_1 . Then \mathbf{y}_t can be partitioned into m blocks of dimension n_1, \dots, n_m , and for each blocks are valid the considerations done for the previous case.

To obtain a positive moving average filter as linear combination of the elements of \mathbf{y}_t it is sufficient to choose $\mathbf{w} \in \mathbb{R}^p$ such that $\mathbf{w}^T \mathbf{b} = 1$ and, partitioning \mathbf{w} into blocks of dimension n_1, \dots, n_m , the elements of each block in decreasing order with the first one being positive. Note that $\mathbf{w}^T \mathbf{b}$ is the sum of the first elements of those blocks.

With the interpretation of the elements \mathbf{y}_t , or their linear combinations, as deviations of ξ_t from different moving averages, it turns out that the instantaneous variance is a quadratic function of those offset processes. Let assume that we want σ_t^2 to be a quadratic function of the set of offsets $\mathbf{w}_1^T \mathbf{y}_t, \dots, \mathbf{w}_r^T \mathbf{y}_t$, for some vectors $\mathbf{w}_1, \dots, \mathbf{w}_r \in \mathbb{R}^p$, $1 \leq r$. Then,

$$\sigma_t^2 = \alpha + 2\beta_0^T \mathbf{W}^T \mathbf{y}_t + \mathbf{y}_t^T \mathbf{W} \mathbf{\Gamma}_0 \mathbf{W}^T \mathbf{y}_t, \quad (12)$$

for some $\alpha > 0$, $\beta_0 \in \mathbb{R}^r$ and $\mathbf{\Gamma}_0 \in \mathcal{S}_+^r$, and where $\mathbf{W} \in \mathbb{R}^{p \times r}$ is the matrix with columns $\mathbf{w}_1, \dots, \mathbf{w}_r$. This is exactly the model presented in (6c), where $\beta = \mathbf{W} \beta_0$ and $\mathbf{\Gamma} = \mathbf{W} \mathbf{\Gamma}_0 \mathbf{W}^T$.

2.4. Conditional moments

In the following, additional assumptions will be imposed to guarantee that the first two conditional moments of σ_t^2 do not diverge as $t \rightarrow \infty$. This property implies that the model allows for weak-stationarity of the variance process.

To this aim, rewrite the variance function as

$$\sigma_t^2 = \alpha + 2\beta^T \mathbf{y}_t + \gamma^T \mathbf{q}_t, \quad (13)$$

where $\gamma = \text{Vec}(\Gamma)$ and $\mathbf{q}_t = (\mathbf{y}_t \otimes \mathbf{y}_t)$. Then,

$$\mathbb{E}[\sigma_t^2 \mid \mathcal{F}_0] = \alpha + 2\beta^T \mathbf{m}_0^{(1)}(t) + \gamma^T \mathbf{m}_0^{(2)}(t),$$

where $\mathbf{m}_0^{(1)}(t) = \mathbb{E}[\mathbf{y}_t \mid \mathcal{F}_0]$ and $\mathbf{m}_0^{(2)}(t) = \mathbb{E}[\mathbf{q}_t \mid \mathcal{F}_0]$. The following result provides a characterisation of the conditional first four moments of \mathbf{y}_t , or, equivalently, of the first two moments of $(\mathbf{y}_t; \mathbf{q}_t)$.

The following Lemma characterises the conditional moments and marginal moments

$$\mathbf{m}_0^{(k)}(t) = \mathbb{E}[\mathbf{y}_{t+s}^{\otimes k} \mid \mathcal{F}_0], \quad \mathbf{m}^{(k)}(t) = \mathbb{E}[\mathbf{y}_{t+s}^{\otimes k}], \quad k = 1, \dots,$$

as functions of $t \in [0, T-s]$ for a fixed $s \geq 0$. Next, a corollary provides an analogous result for the marginal moments $\mathbf{m}^{(k)}(t) = \mathbb{E}[\mathbf{y}^{\otimes k}]$. In the following, the derivative of $f(t)$ w.r.t. its arguments is represented by $\dot{f}(t) = df(t)/dt$.

Lemma 2 *If Assumption 1 holds, then $\mathbf{m}_0 = (\mathbf{m}_0^{(1)}; \mathbf{m}_0^{(2)}; \mathbf{m}_0^{(3)}; \mathbf{m}_0^{(4)})$ is solution to the lower block-triangular ODE*

$$\underbrace{\begin{pmatrix} \dot{\mathbf{m}}_0^{(1)} \\ \dot{\mathbf{m}}_0^{(2)} \\ \dot{\mathbf{m}}_0^{(3)} \\ \dot{\mathbf{m}}_0^{(4)} \end{pmatrix}}_{\dot{\mathbf{m}}_0} = \underbrace{\begin{pmatrix} 0 \\ \alpha \bar{\mathbf{b}} \\ 0 \\ 0 \end{pmatrix}}_{\mathbf{a}} - \underbrace{\begin{pmatrix} \mathbf{A}_{11} & 0 & 0 & 0 \\ \mathbf{A}_{21} & \mathbf{A}_{22} & 0 & 0 \\ \mathbf{A}_{31} & \mathbf{A}_{32} & \mathbf{A}_{33} & 0 \\ 0 & \mathbf{A}_{42} & \mathbf{A}_{43} & \mathbf{A}_{44} \end{pmatrix}}_{\mathbf{A}} \underbrace{\begin{pmatrix} \mathbf{m}_0^{(1)} \\ \mathbf{m}_0^{(2)} \\ \mathbf{m}_0^{(3)} \\ \mathbf{m}_0^{(4)} \end{pmatrix}}_{\mathbf{m}_0}, \quad \text{on } [0, T], \quad (14)$$

with initial condition

$$\mathbf{m}_0^{(k)}(0) = \mathbf{y}_0^{\otimes k}, \quad k = 1, 2, 3, 4, \quad (15)$$

where $\bar{\mathbf{b}} = \mathbf{b} \otimes \mathbf{b}$ and the blocks of \mathbf{A} are given by

$$\mathbf{A}_{kk} = \mathbf{A}^{(k)} - \mathbf{B}^{(k)} \otimes \gamma^T, \quad \mathbf{A}_{k,k-1} = -2\mathbf{B}^{(k)} \otimes \beta^T, \quad \mathbf{A}_{k,k-2} = -\alpha \mathbf{B}^{(k)}, \quad (16)$$

with $\mathbf{A}^{(k)}$, $\mathbf{B}^{(k)}$ and $\mathbf{C}^{(k)}$ recursively given by

$$\mathbf{A}^{(1)} = \mathbf{A}, \quad \mathbf{A}^{(k+1)} = \mathbf{I}_p \otimes \mathbf{A}^{(k)} + \mathbf{A} \otimes \mathbf{I}_{p^k}, \quad k \geq 1, \quad (17a)$$

$$\mathbf{B}^{(1)} = 0, \quad \mathbf{B}^{(k+1)} = \mathbf{I}_p \otimes \mathbf{B}^{(k)} + \mathbf{b} \otimes \mathbf{C}^{(k)}, \quad k \geq 1, \quad (17b)$$

$$\mathbf{C}^{(1)} = \mathbf{b}, \quad \mathbf{C}^{(k+1)} = \mathbf{I}_p \otimes \mathbf{C}^{(k)} + \mathbf{b} \otimes \mathbf{I}_{p^k}. \quad k \geq 1, \quad (17c)$$

Moreover, $\mathbf{m} = (\mathbf{m}^{(1)}; \mathbf{m}^{(2)}; \mathbf{m}^{(3)}; \mathbf{m}^{(4)})$ solves the ODE (14) with initial condition $\mathbf{m}^{(k)}(0) = \mathbb{E}[\mathbf{y}_0^{\otimes k}]$, $k = 1, 2, 3, 4$.

When \mathbf{A} is non-singular,

$$\mathbf{m}_0(t) = (\mathbf{I} - e^{-\mathbf{A}t})\mathbf{m}_\infty + e^{-\mathbf{A}t}\mathbf{m}_0(0),$$

and

$$\mathbf{m}(t) = (\mathbf{I} - e^{-\mathbf{A}t})\mathbf{m}_\infty + e^{-\mathbf{A}t}\mathbf{m}(0),$$

where $\mathbf{m}_\infty = \mathbf{A}^{-1}\mathbf{a}$.

PROOF See Appendix A. ■

Regarding the structure of the matrix \mathbf{A} defined in (14), note that $\bar{\mathbf{b}} = \mathbf{B}^{(2)}$, $\bar{\mathbf{A}} = \mathbf{A}^{(2)} = \mathbf{A} \otimes \mathbf{I}_p + \mathbf{I}_p \otimes \mathbf{A}$ and the top-left sub-matrix of \mathbf{A} is given by

$$\tilde{\mathbf{A}} = \begin{pmatrix} \mathbf{A}_{11} & 0 \\ \mathbf{A}_{21} & \mathbf{A}_{22} \end{pmatrix} = \begin{pmatrix} \mathbf{A} & 0 \\ -2\bar{\mathbf{b}}\boldsymbol{\beta}^T & \bar{\mathbf{A}} - \bar{\mathbf{b}}\boldsymbol{\gamma}^T \end{pmatrix}. \quad (18)$$

Moreover, from the structure of \mathbf{A} and \mathbf{a} it follows that the first block of \mathbf{m}_∞ is zero ($\mathbf{m}_\infty^{(1)} = 0$) and the second block, hereafter denoted by \mathbf{q}_∞ , is given by

$$\mathbf{q}_\infty = \mathbf{m}_\infty^{(2)} = \alpha \mathbf{A}_{22}^{-1} \bar{\mathbf{b}} = (1 - \kappa)^{-1} \alpha \bar{\mathbf{A}}^{-1} \bar{\mathbf{b}}, \quad \kappa = \boldsymbol{\gamma}^T \bar{\mathbf{A}}^{-1} \bar{\mathbf{b}}. \quad (19)$$

Since the coefficient matrix \mathbf{A} is block triangular, the stability of the ODE (14) is determined by the eigenvalues of the diagonal blocks. More precisely, that ODE is stable when all the eigenvalues of \mathbf{A}_{22} , \mathbf{A}_{33} and \mathbf{A}_{44} have positive real part. In the following Lemma a sufficient condition for that stability is provided.

Lemma 3 (Stability of models with non-negative hessian $\boldsymbol{\Gamma}$) *Under Assumptions 1 and 2, if*

$$\boldsymbol{\Gamma} \geq 0 \quad \text{and} \quad \tilde{\kappa} = \lambda_{\min} \mathbf{b}^T \mathbf{A}^{-T} \boldsymbol{\Gamma} \mathbf{A}^{-1} \mathbf{b} < \frac{2}{3}, \quad (20)$$

then all the eigenvalues of \mathbf{A} have positive real part.

PROOF See Appendix A. ■

2.5. Autocovariance function and Weak stationarity of the variance process

When all the eigenvalues of \mathbf{A} have positive real part the ODE is stable, and one can consider to expand the horizon of the solutions: $T \rightarrow \infty$. In that case, $\lim_{t \rightarrow \infty} \mathbf{m}_0(t) = \mathbf{m}_\infty$. Moreover, if the distribution of \mathbf{y}_0 has the first two moments given by $\mathbf{m}_\infty^{(1)}$ and $\mathbf{m}_\infty^{(2)}$, then the process \mathbf{y}_t will be weak-stationary. Being a linear function of \mathbf{y}_t and $\mathbf{y}_t^{\otimes 2}$, the variance process σ_t^2 is weak-stationary when the moments up to the fourth order of \mathbf{y}_0 are given by \mathbf{m}_∞ .

The following assumption is related to the stability of the SDE (14) and to the weak-stationarity of both the offset process \mathbf{y}_t and the variance process σ_t^2 .

Assumption 3 (Weak stationarity of the variance process) *The eigenvalues of \mathbf{A}_{kk} , $1 \leq k \leq 4$ have strictly positive real parts and the first fourth-order moments of \mathbf{y}_0 are given by $\mathbf{m}_\infty = \mathbf{A}^{-1}\mathbf{a}$.*

Consider the $p + p^2$ dimensional process $\boldsymbol{\eta}_t = (\mathbf{y}_t; \mathbf{q}_t)$, $\mathbf{q}_t = \mathbf{y}_t \otimes \mathbf{y}_t$. Clearly, the first four moments of \mathbf{y}_t correspond to the first two moments of $\boldsymbol{\eta}_t$ and, thus, $\mathbf{m}(t)$ contains those moments. It follows that, under Assumptions 1 and 3, since $\mathbf{m}(0) = \mathbf{m}_\infty$, the first two moments of $\boldsymbol{\eta}_t$ have mean and variance that do not depend on t :

$$\mathbb{E}[\boldsymbol{\eta}] = \boldsymbol{\eta}_\infty = \begin{pmatrix} 0 \\ \mathbf{q}_\infty \end{pmatrix}, \quad \text{and} \quad \mathbb{E}[\boldsymbol{\eta}_t \boldsymbol{\eta}_t^T] = \begin{pmatrix} \mathbf{M}_2 & \mathbf{M}_3 \\ \mathbf{M}_3^T & \mathbf{M}_4 \end{pmatrix}, \quad (21)$$

where $\mathbf{M}_2 \in \mathbb{R}^{p \times p}$, $\mathbf{M}_3 \in \mathbb{R}^{p \times p^2}$ and $\mathbf{M}_4 \in \mathbb{R}^{p^2 \times p^2}$ are such that $\text{Vec}(\mathbf{M}_k) = \mathbf{m}_\infty^{(k)}$, $k = 2, 3, 4$. It follows that the covariance matrix of $\boldsymbol{\eta}_t$ is

$$\text{Cov}(\boldsymbol{\eta}_t) = \boldsymbol{\Omega} = \begin{pmatrix} \mathbf{M}_2 & \mathbf{M}_3 \\ \mathbf{M}_3^T & \mathbf{M}_4 - \mathbf{q}_\infty \mathbf{q}_\infty^T \end{pmatrix}. \quad (22)$$

We will not continue to seek an explicit expression for \mathbf{M}_3 and \mathbf{M}_4 , as these are more complex to implement than simply solving the block-triangular system $\mathbf{A}\mathbf{m}_\infty = \mathbf{a}$ numerically.

Proposition 1 (Conditional expectation) *Under Assumption 1, if \mathbf{A} is non-singular, then*

$$\mathbb{E}[\boldsymbol{\eta}_{t+s} \mid \mathcal{F}_t] = \boldsymbol{\eta}_\infty + e^{-\tilde{\mathbf{A}}s}(\boldsymbol{\eta}_s - \boldsymbol{\eta}_\infty), \quad (23)$$

where $\boldsymbol{\eta}_\infty$ and $\tilde{\mathbf{A}}$ are defined in (21) and (18), respectively. Moreover, the conditional instantaneous variance is given by

$$v_t(s) = \mathbb{E}[\sigma_{t+s}^2 \mid \mathcal{F}_t] = \sigma_\infty^2 + \boldsymbol{\psi}(s)^T(\boldsymbol{\eta}_t - \boldsymbol{\eta}_\infty), \quad (24)$$

where

$$\sigma_\infty^2 = \frac{\alpha}{1 - \kappa}, \quad \boldsymbol{\psi}(s) = (e^{-\tilde{\mathbf{A}}s})^T \mathbf{g}, \quad \mathbf{g}^T = (2\boldsymbol{\beta}^T \ \boldsymbol{\gamma}^T), \quad (25)$$

and κ is defined in (19).

PROOF The first result is a direct consequence of Lemma 2. The second one, follows by rewriting the variance as an affine combination of $\boldsymbol{\eta}_t$: $\sigma_t^2 = \alpha + \mathbf{g}^T \boldsymbol{\eta}_t$. \blacksquare

Lemma 4 (Weak stationarity of $\boldsymbol{\eta}_t$ and σ_t^2) *If Assumptions 1 and 3 hold, then the process $\boldsymbol{\eta}_t$ is weak-stationary with expectation $\boldsymbol{\eta}_\infty$ and covariance matrix $\boldsymbol{\Omega}$ given, respectively, in (21) and auto-covariance function*

$$s \rightarrow \text{Cov}(\boldsymbol{\eta}_{t+s}, \boldsymbol{\eta}_t^T) = e^{-\tilde{\mathbf{A}}s} \boldsymbol{\Omega}, \quad (26)$$

where $\tilde{\mathbf{A}}$ is defined in (18).

Moreover, the process σ_t^2 is weak-stationary with

$$\mathbb{E}[\sigma_t^2] = \sigma_\infty^2, \quad \text{and} \quad \mathbb{E}[\sigma_t^4] = \alpha + \mathbf{g}^T \boldsymbol{\Omega} \mathbf{g},$$

and autocovariance function given by

$$s \rightarrow \text{Cov}(\sigma_{t+s}^2, \sigma_t^2) = \boldsymbol{\psi}(s)^T \boldsymbol{\Omega} \mathbf{g}, \quad (27)$$

where σ_∞^2 , $\boldsymbol{\psi}(s)$ and \mathbf{g} are defined in (25).

PROOF Note that the first two order moments of $\boldsymbol{\eta}_t$ corresponds to the first four order moments of \mathbf{y}_t . Then, since from Assumption 3 all the eigenvalues of \mathbf{A} have positive real part, the weak stationarity of $\boldsymbol{\eta}_t$ is a direct consequence of Lemma 2.

Next, to obtain (26), apply the decomposition of variance rule and (24):

$$\text{Cov}(\boldsymbol{\eta}_{t+s}, \boldsymbol{\eta}_t^T) = \underbrace{\text{Cov}(\mathbb{E}[\boldsymbol{\eta}_{t+s} | \mathcal{F}_t], \boldsymbol{\eta}_t)}_{=\text{Cov}(e^{-\tilde{\mathbf{A}}s} \boldsymbol{\eta}_t, \boldsymbol{\eta}_t)} + \underbrace{\mathbb{E}[\text{Cov}(\boldsymbol{\eta}_{t+s}, \boldsymbol{\eta}_t^T | \mathcal{F}_t)]}_{=0} = e^{-\tilde{\mathbf{A}}s} \boldsymbol{\Omega}. \quad \blacksquare$$

The remaining results follow by recalling that $\sigma_t^2 = \alpha + \mathbf{g}^T \boldsymbol{\eta}_t$.

Being σ_∞^2 the log-return's variance, the corresponding Kurtosis is defined as

$$\text{Kurt}_\infty = \mathbb{E}[\sigma_t^4] / \sigma_\infty^4. \quad (28)$$

Remark 2 One implication of these considerations is that, although the dynamics specification of \mathbf{y}_t involve only the m roots $\lambda_1, \dots, \lambda_m$, the feedback due to dependence of the volatility coefficient on \mathbf{y}_t induces additional artificial roots on the auto-correlation structure of the processes \mathbf{y}_t and, in turn, σ_t^2 . \square

2.6. Forward variance term structure and its principal component decomposition

From a financial point of view, when the SDEs (6a)-(6b) correspond to the discounted log-price's risk-neutral dynamics, the conditional variance $v_t(s)$ represents the “forward instantaneous variance”, or simply “forward variance”, for the maturity $t + s$. Note that, seen as function of \mathbf{y}_t , $v_t(s)$ is quadratic, while seen as function of $\boldsymbol{\eta}_t$, v_t is affine [14]. Then, the forward variance curve can be decomposed into a fixed term, a linear combination of the factors \mathbf{y}_t and one of their “interactions” $\mathbf{q}_t = \mathbf{y}_t \otimes \mathbf{y}_t$:

$$\begin{aligned} v_t(s) &= v^0(s) + \sum_{i=1}^p \psi_i^{(\mathbf{y})}(s) y_{it} + \sum_{i,j=1}^p \psi_{i,j}^{(\mathbf{Q})}(s) y_{it} y_{jt} \\ &= v^0(s) + \mathbf{y}_t^T \boldsymbol{\psi}^{(\mathbf{y})}(s) + \mathbf{y}_t^T \boldsymbol{\Psi}^{(\mathbf{Q})}(s) \mathbf{y}_t. \end{aligned} \quad (29)$$

Here, $\boldsymbol{\psi}^{(\mathbf{y})}$ corresponds to the first p elements of $\boldsymbol{\psi}$, while $\boldsymbol{\Psi}^{(Q)}$ to the last p^2 . Clearly, as the coefficients of the quadratic function $\mathbf{y}_t \rightarrow v_t(s)$ are functions of the time-to-maturity s , also its minimum depend on s . More precisely,

$$v^{\min}(s) = \min_{\mathbf{y}_t} v_t(s) = v^0(s) + \frac{1}{4} \boldsymbol{\psi}^{(\mathbf{y})}(s)^T (\boldsymbol{\Psi}^{(Q)}(s))^{-1} \boldsymbol{\psi}^{(\mathbf{y})}(s), \quad s, t \geq 0. \quad (30)$$

Moreover, since $v_t(s) \rightarrow v_\infty$ as $s \rightarrow \infty$, that convex function of \mathbf{y}_t asymptotically flattens to the stationary level. Some instances of the curves v^0 and v^{\min} are shown in Figure 8.

Since the decomposition in (29) depends on the parameterisation, it is be more appropriate to consider a principal component decomposition that depend only on the first two moments of the forward variance curve $v_t(s)$. The following proposition describes an algorithm for obtaining the factors of such decomposition.

Proposition 2 (Principal Component decomposition of the Forward Variance curve)

If Assumptions 1 and 3 hold, then the principal component decomposition of the forward variance curve $v_t(\cdot)$ is given by

$$\text{Cov}(v_t(s_1), v_t(s_2)) = \mathbf{u}(s_1)^T \mathbf{D} \mathbf{u}(s_2), \quad t, s_1, s_2 \geq 0, \quad (31a)$$

$$\int_0^\infty \mathbf{u}(t) \mathbf{u}(t)^T dt = \mathbf{I}. \quad (31b)$$

where the diagonal matrix with the eigenvalues $\text{diag}(\mathbf{D})$ and the principal factors vector $\mathbf{u}(\cdot)$ are defined as follows.

Let $\mathbf{R} \in \mathbb{R}^{(p+p^2) \times r}$ be a Cholesky factor of

$$\mathbf{F} = \int_0^\infty \boldsymbol{\psi}(t) \boldsymbol{\psi}(t)^T dt = \mathbf{R} \mathbf{R}^T, \quad (32)$$

where $1 \leq r \leq (p+p^2)$ is the rank of \mathbf{F} and \mathbf{R} has full rank. Next, consider the eigenvalue decomposition of $\mathbf{R}^T \boldsymbol{\Omega} \mathbf{R}$, with $\boldsymbol{\Omega}$ being the covariance matrix defined in (22):

$$\mathbf{R}^T \boldsymbol{\Omega} \mathbf{R} = \mathbf{V} \mathbf{D} \mathbf{V}^T,$$

where $\mathbf{V}, \mathbf{D} \in \mathbb{R}^{r \times r}$, \mathbf{V} orthogonal and $\mathbf{D} \geq 0$ diagonal. Finally, define $\mathbf{u} : \mathbb{R}_+ \rightarrow \mathbb{R}^r$ as

$$\mathbf{u}(t) = \mathbf{V}^T \mathbf{R}^+ \boldsymbol{\psi}(t),$$

where $\mathbf{R}^+ \in \mathbb{R}^{r \times (p+p^2)}$ is a pseudo-inverse of \mathbf{R} such that $\mathbf{R}^+ \mathbf{R} = \mathbf{I}_r$.

PROOF Firstly, by Assumptions 1 and 3 all the eigenvalues of $\tilde{\mathbf{A}}$ have positive real part, and, since $\boldsymbol{\psi}(t) = (e^{-\tilde{\mathbf{A}}s})^T \mathbf{g}$, the integral in (32) is finite. Moreover, the covariance matrix $\boldsymbol{\Omega}$ is well defined. Now, since the integrand in (32) is positive semidefinite, it is necessary that $\boldsymbol{\psi}(t)$ belong to the column range of \mathbf{R} for all $t \geq 0$. It follows that $\boldsymbol{\psi}(t) = \mathbf{R} \mathbf{V} \mathbf{u}(t)$. Finally, by (24) and (22), for $t, s_1, s_2 \geq 0$,

$$\text{Cov}(v_t(s_1), v_t(s_2)) = \boldsymbol{\psi}(s_1)^T \boldsymbol{\Omega} \boldsymbol{\psi}(s_2) = \mathbf{u}(s_1)^T \mathbf{V}^T \mathbf{R} \boldsymbol{\Omega} \mathbf{R} \mathbf{V} \mathbf{u}(s_2) = \mathbf{u}(s_1)^T \mathbf{D} \mathbf{u}(s_2). \quad \blacksquare$$

Remark 3 Note that, $\boldsymbol{\eta}_t = (\mathbf{y}_t; \text{Vec}(\mathbf{Q}_t))$ where $\mathbf{Q}_t = \mathbf{y}_t \mathbf{y}^T$ is symmetric. Then, $p(p-1)$ elements of $\boldsymbol{\eta}_t$ have an identical copy. It follows that the covariance matrix $\boldsymbol{\Omega}$ has $p(p-1)/2$ null eigenvalues, and the number of factors in the PCA (31) can be reduced to $p(p+3)/2$ without any loss of information. ■

Remark 4 The integral in (32) can be explicitly computed in terms of the matrix $\tilde{\mathbf{A}}$ as follows. Since $\boldsymbol{\psi}(t) = (e^{-\tilde{\mathbf{A}}t})^T \mathbf{g}$, the integrand can be rewritten as

$$\text{Vec}(\boldsymbol{\psi}(t)\boldsymbol{\psi}(t)^T) = \boldsymbol{\psi}(t) \otimes \boldsymbol{\psi}(t) = (e^{-\tilde{\mathbf{A}}t} \otimes e^{-\tilde{\mathbf{A}}t})^T (\mathbf{g} \otimes \mathbf{g}) = (e^{-(\tilde{\mathbf{A}} \otimes \mathbf{I} + \mathbf{I} \otimes \tilde{\mathbf{A}})t})^T (\mathbf{g} \otimes \mathbf{g}),$$

and, thus,

$$\begin{aligned} \text{Vec}(F) &= - \left[(\tilde{\mathbf{A}} \otimes \mathbf{I} + \mathbf{I} \otimes \tilde{\mathbf{A}})^{-1} (e^{-(\tilde{\mathbf{A}} \otimes \mathbf{I} + \mathbf{I} \otimes \tilde{\mathbf{A}})t})^T (\mathbf{g} \otimes \mathbf{g}) \right]_0^\infty \\ &= (\tilde{\mathbf{A}} \otimes \mathbf{I} + \mathbf{I} \otimes \tilde{\mathbf{A}})^{-1} (\mathbf{g} \otimes \mathbf{g}). \end{aligned}$$

That is, \mathbf{F} solves the matrix equation $\tilde{\mathbf{A}}^T \mathbf{F} + \mathbf{F} \tilde{\mathbf{A}} = \mathbf{g} \mathbf{g}^T$. ■

2.7. The autocorrelation of squared increments

Following [3], consider the increment process

$$\xi_t^{(r)} = \xi_{t+r} - \xi_t, \quad \xi_t = \int_0^t \sigma_s dW_s.$$

The following Lemma characterises the autocorrelation structure of the increment and squared increment processes $\xi_t^{(r)}$ and $(\xi_t^{(r)})^2$.

Lemma 5 *If Assumptions 1 and 3 hold, then for any $t \geq 0$ and $h \geq r \geq 0$,*

$$\begin{aligned} \mathbb{E}[\xi_t^{(r)}] &= 0, & \text{Cov}(\xi_t^{(r)}, \xi_{t+h}^{(r)}) &= 0, \\ \mathbb{E}[(\xi_t^{(r)})^2] &= r\sigma_\infty^2, & \text{Cov}((\xi_t^{(r)})^2, (\xi_{t+h}^{(r)})^2) &= \mathbf{g}^T e^{-\tilde{\mathbf{A}}h} \mathbf{h}_r, \end{aligned}$$

where

$$\mathbf{h}_r = \tilde{\mathbf{A}}^{-1} (e^{\tilde{\mathbf{A}}r} - \mathbf{I}) \text{Cov}(\boldsymbol{\eta}_r, \xi_r^2).$$

PROOF Without loss of generality assume $t = 0$. The null expectation of $\xi_0^{(r)}$ is a direct consequence of its definition. Consider its variance,

$$\mathbb{E}[(\xi_0^{(r)})^2] = \mathbb{E}[\xi_r^2] = \mathbb{E} \left[\left(\int_0^r \sigma_s dW_s \right)^2 \right] = r\sigma_\infty^2,$$

since the process σ_s^2 is stationary with expectation σ_∞^2 . Next,

$$\text{Cov}(\xi_0^{(r)}, \xi_h^{(r)}) = \mathbb{E}[\xi_0^{(r)} \xi_h^{(r)}] = \mathbb{E} [\xi_0^{(r)} \mathbb{E}[\xi_h^{(r)} | \mathcal{F}_h]] = 0.$$

Finally, to obtain the expression for the autocovariance function of squared increments, note that by (24)

$$\begin{aligned} \mathbb{E}[(\xi_h^{(r)})^2 \mid \mathcal{F}_r] &= \mathbb{E} \left[\int_h^{h+r} \sigma_s^2 ds \mid \mathcal{F}_r \right] = \int_{h-r}^h v_r(s) ds \\ &= r\sigma_\infty^2 + \int_{h-r}^h \psi(s)^T (\boldsymbol{\eta}_r - \boldsymbol{\eta}_\infty) ds \\ &= r\sigma_\infty^2 + \mathbf{g}^T e^{-\tilde{\mathbf{A}}h} \tilde{\mathbf{A}}^{-1} (e^{\tilde{\mathbf{A}}r} - \mathbf{I}) (\boldsymbol{\eta}_r - \boldsymbol{\eta}_\infty). \end{aligned}$$

Now, since $\xi_0^r = \xi_r$, $\mathbb{E}[(\xi_0^{(r)})^2 (\xi_h^{(r)})^2] = \mathbb{E}[\xi_r^2 (\xi_h^{(r)})^2]$ and thus

$$\begin{aligned} \mathbb{E}[(\xi_0^{(r)})^2 (\xi_h^{(r)})^2] &= \mathbb{E} \left[\xi_r^2 \mathbb{E}[(\xi_h^{(r)})^2 \mid \mathcal{F}_r] \right] \\ &= r\sigma_\infty^2 \mathbb{E}[\xi_r^2] + \mathbf{g}^T e^{-\tilde{\mathbf{A}}h} \tilde{\mathbf{A}}^{-1} (e^{\tilde{\mathbf{A}}r} - \mathbf{I}) \mathbb{E}[\xi_r^2 (\boldsymbol{\eta}_r - \boldsymbol{\eta}_\infty)] \\ &= (r\sigma_\infty^2)^2 + \mathbf{g}^T e^{-\tilde{\mathbf{A}}h} \tilde{\mathbf{A}}^{-1} (e^{\tilde{\mathbf{A}}r} - \mathbf{I}) \text{Cov}(\boldsymbol{\eta}_r, \xi_r^2). \quad \blacksquare \end{aligned}$$

3. Specific models and numerical tests

3.1. Scalar QHR model

When $p = m = n = 1$, the SDE (6b) can be rewritten as

$$dy_t = -\lambda y_t dt + \sigma_t dW_t, \quad \sigma_t^2 = \alpha + 2\beta y_t + \gamma y_t^2, \quad (33)$$

where $\lambda, \alpha > 0$ and $\beta, \gamma \in \mathbb{R}$ are such that $\gamma\alpha > \beta^2$. The variance function is quadratic function whose minimum is located at $y_{\min} = -\gamma/\beta$ and has value $\sigma_{\min}^2 = \alpha^2 - \gamma/\beta^2$.

The variance is function of the offset from an exponential moving average with coefficient λ on the trajectory of the detrended log-return ξ_t . The process $\boldsymbol{\eta}_t = (y_t; q_t)$ has dynamics

$$\boldsymbol{\eta}_t = -\tilde{\mathbf{A}}(\boldsymbol{\eta}_t - \boldsymbol{\eta}_\infty)dt + \begin{pmatrix} 1 \\ 2y_t \end{pmatrix} \sigma_t dW_t, \quad \tilde{\mathbf{A}} = \begin{pmatrix} \lambda & 0 \\ -2\beta & 2\lambda - \gamma \end{pmatrix}, \quad \boldsymbol{\eta}_\infty = \begin{pmatrix} 0 \\ q_\infty \end{pmatrix},$$

and where $q_\infty = \alpha/(2\lambda(1 - \kappa))$, $\kappa = \gamma/(2\lambda)$. The mean reversion level for σ_t^2 is given by $\sigma_\infty^2 = \alpha/(1 - \kappa) = 2\alpha\lambda/(2\lambda - \gamma)$. Moreover, \mathbf{A}_{33} and \mathbf{A}_{44} are scalar and their values are given by

$$\mathbf{A}_{33} = 3\lambda - 2\gamma, \quad \mathbf{A}_{44} = 4\lambda - 6\gamma.$$

It follows that the stability condition becomes

$$\gamma < 2\lambda/3.$$

Note that, the constants κ and $\tilde{\kappa}$ defined in (19) and (20) are given by $\kappa = \gamma/(2\lambda)$ and $\tilde{\kappa} = \gamma/\lambda$.

Thus, the variance process has two roots, with values λ and $2\lambda - \gamma$. When the stability condition, the additional root belongs to the range $[4\lambda/3, 2\lambda]$.

Note that, for the stationary solution, $y_\infty = E[y_t] = 0$ but $\sigma_\infty^2 = E[\sigma_t^2]$ is different from the value of σ_t^2 when $y_t = 0$. Moreover, if $\beta \neq 0$, the equilibrium value for y_t does not correspond to a minimum volatility level, see Table 1. Note that, the stationary variance linearly depends on the coefficient α and it is also always larger: $\sigma_\infty^2 = \alpha(1 - \kappa) > \alpha$, since $\kappa > 0$.

Table 1: Specific values for y_t and σ_t

Description of state	y_t	q_t	σ_t^2
y_t at mean-reversion level	0	0	α
y_t at stationary distribution	0	q_∞	σ_∞^2
y_t at minimum spot-variance	$-\beta/\gamma$	0	$\alpha - \beta^2/\gamma$

Some computations lead to the following expressions for $m_\infty^{(3)}$ and $m_\infty^{(4)}$, respectively, the third and fourth order moments of y_t under the weak-stationary distribution,

$$m_\infty^{(3)} = \frac{2\beta}{\lambda - \gamma} q_\infty, \quad m_\infty^{(4)} = 3 \frac{2\lambda - \gamma}{2\lambda - 3\gamma} \left(1 + 4 \frac{\beta^2}{\alpha(\lambda - \gamma)} \right) q_\infty^2.$$

Clearly, the parameter β directly controls the asymmetry of the distribution of y_t .

It can be shown, that under stationarity, the returns Kurtosis defined in (28) is given by

$$\text{Kurt}_\infty = \frac{2\lambda - \gamma}{2\lambda - 3\gamma} \left(\frac{\lambda - \gamma}{\lambda} + \frac{2\lambda - \gamma}{\lambda - \gamma} \frac{\beta^2}{\lambda\alpha} \right), \quad (34)$$

W.r.t. β , that kurtosis is minimal when $\beta = 0$, maximal when $\beta^2 = \gamma\alpha$. Thus, the following bound hold:

$$\frac{2\lambda - \gamma}{2\lambda - 3\gamma} \frac{\lambda - \gamma}{\lambda} \leq \text{Kurt}_\infty \leq \frac{\lambda}{\lambda - \gamma} \frac{2\lambda - \gamma}{2\lambda - 3\gamma}.$$

Note also that Kurt_∞ has the following homogeneity property

$$\text{Kurt}_\infty = \frac{2 - \tilde{\gamma}}{2 - 3\tilde{\gamma}} \left(1 - \tilde{\gamma} + \frac{2 - \tilde{\gamma}}{1 - \tilde{\gamma}} \frac{\tilde{\beta}^2}{\tilde{\alpha}} \right), \quad (35)$$

where $\tilde{\alpha} = \alpha/\lambda$, $\tilde{\beta} = \beta/\lambda$ and $\tilde{\gamma} = \gamma/\lambda$. The upper- and lower-bound given in (35) are shown in subsection 3.1. Notice that, the value of γ/λ is the main driver for the Kurtosis and that any possible value of the kurtosis can be obtained by this model.

Resuming, the stationary distribution of the scalar model has the following qualitative behaviour:

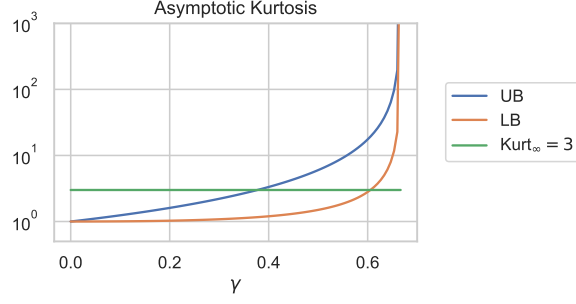


Figure 2: The upper- (UB) and lower-bound (LB) of the asymptotic Kurtosis given in (35) as function of γ , when $\lambda = 1$. The green horizontal line represents the mesokurtic level.

- under stationarity, expectation does not corresponds to minimum volatility unless $\beta = 0$;
- asymmetry of y_t is directly proportional to β ;
- return's kurtosis is an increasing function of γ and of β^2/α .

Proposition 3 (Stationary distribution of the scalar QHR model) *When $\Delta = \alpha\gamma - \beta^2 > 0$ and $\gamma < 2\lambda/3$, the SDE (33) has a stationary solution given by a Pearson type IV distribution. More precisely, the stationary distribution y_∞ has probability density function (PDF) given by*

$$p_{y_\infty}(y) = P[y_\infty \in dy] = C(\alpha + 2\beta y + \gamma y^2)^{-\frac{\lambda}{\gamma}-1} \exp\left(\frac{2\lambda\beta/\gamma}{\sqrt{\Delta}} \arctan\left(\frac{\beta + \gamma y}{\sqrt{\Delta}}\right)\right),$$

where C is a normalisation constant.

In particular, when $\beta = 0$, y_∞ is proportional to a Student- t random variable with $2\lambda/\gamma + 1$ degrees of freedom:

$$\sqrt{\frac{\alpha}{2\lambda + \gamma}} y_\infty \sim \text{Student-}t(2\lambda/\gamma + 1).$$

PROOF It is direct to verify that p_{y_∞} is positive and solves the Pearson equation

$$\frac{p'(y)}{p(y)} = -2 \frac{\beta + (\lambda + \gamma)y}{\alpha + 2\beta y + \gamma y^2}$$

(see [22, 25]). The latter can be rewritten as

$$\frac{1}{2} \partial_y (\sigma^2(y) p(y)) + \lambda y p(y) = 0.$$

It follows that $p(y, t) = p_{y_\infty}(y)$ is a constant in time solution to the Fokker-Planck equation (33):

$$\frac{1}{2} \partial_{yy} (\sigma^2(y) p(y, t)) + \partial_y (\lambda y p(y, t)) = \partial_t p(y, t).$$

Thus, p_{y_∞} is the density of a stationary distribution for the SDE (33). ■

3.1.1. Numerical tests

Table 2: Setups used for the experimental results.

Model	Parameters			Diagnostics					
	λ	α	β	γ	$2\lambda - \gamma$	σ_{\min}	\mathbf{y}_{\min}	$\sqrt{v_{\infty}}$	Kurt_{∞}
M_1	6.00	0.0064	0.0000	3.6334	8.37	8.00%	0.00	9.58%	3.00
M_2	4.00	0.0064	0.0000	2.0000	6.00	8.00%	0.00	9.24%	1.50
M_3	6.00	0.0133	-0.1800	3.0000	9.00	5.00%	0.06	13.32%	5.15
M_4	6.00	0.0162	-0.2280	3.8000	8.20	5.00%	0.06	15.39%	32.29

In the rest of this subsection a few examples are tested to show the capabilities of the scalar model. The parameter setup of those models are reported in Table 2. All those models allow for a stationary distribution, since in all the four cases $2\lambda - 3\gamma > 0$. The first two of those models, namely M_1 and M_2 , are symmetrical. All the models have the same exponential parameter $\lambda = 6$, except for M_2 whose parameter is $\lambda = 4$. The non-symmetrical models, namely M_3 and M_4 , have the minimum spot volatility level of 5% is reached when $y_t = 0.06$. Roughly speaking, the market is most quiet when the underlying price is 6% above its exponential moving average. Those two models, despite their lower minimum volatility level, 5% vs 8%, have larger stationary variance and kurtosis than those of the first two models.

Figure 3 shows the forward volatility curves $T \rightarrow \sqrt{v_0(T)}$ of the four models for different values of the initial condition y_0 . Note that the asymmetric models show a richer behaviour with non-necessarily monotone forward curves.

To evaluate the qualitative properties of the scalar QHR when pricing European options, Figure 5 shows the implied volatility smiles for models $M_1 - M_4$. For each model (row), the smiles for different maturities T (color) and different initial conditions \mathbf{y}_0 (column) are plotted in terms of the “Normalised Log-Moneyness” $\log(K/S_0)/\sqrt{T}$. That standardisation has the advantage of letting the smiles more comparable across maturities. To support that statement, compare the first row of Figure 5 with Figure 4 where the same smiles are plotted as function of the plain log-moneyness $\log(K/S_0)$. Recall that, by the homogeneity properties discussed in section 2.2, the pricing function depends only on the K/S_0 and not separately on the underlying price S_0 and strike price K . For this reason all the prices have been computed for an underlying $S_0 = 1$ ($x_0 = 0$). In all those experiments, prices are computed by means of an Euler Monte Carlo method with Antithetic Variables, a time step of $1/250$ and 10^6 scenario. For each model and initial condition, all the prices are computed on the same set of trajectories.

As expected, $\beta \neq 0$ leads to asymmetrical shapes and a larger value of γ , as in models M_1 and M_4 , corresponds to a steeper smile shape. Moreover, in the asymmetric models M_3 and M_4 , when the offset value becomes substantially negative, a larger γ gives higher implied volatilities. Clearly, the smirks obtained by the asymmetrical models M_3 and M_4 more realistically replicate market stylised facts. However, even in those models, as

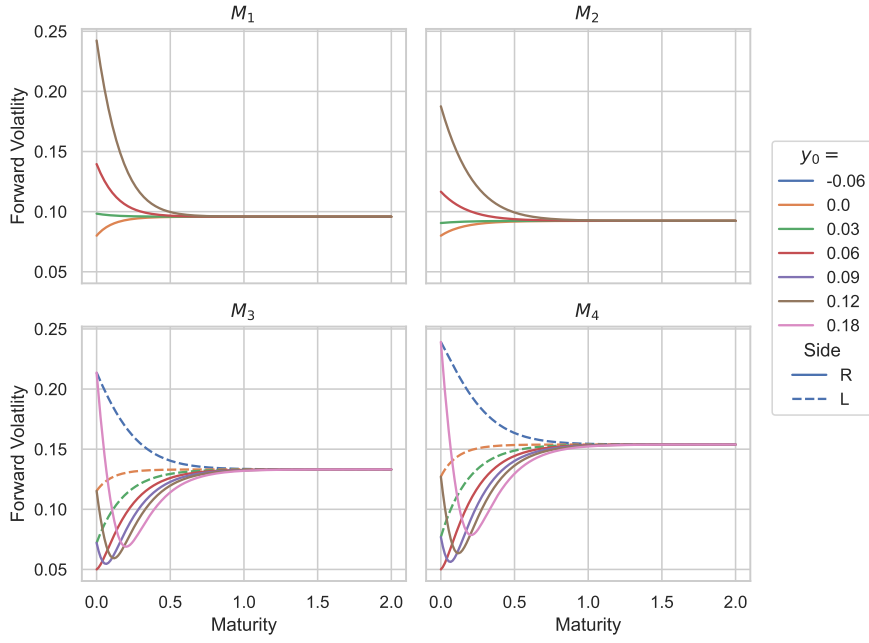


Figure 3: The forward volatility curve $\sqrt{v_0(T)}$ under models M_1, M_2, M_3 and M_4 defined in Table 2. Different colours represent different values for the initial condition y_0 . Solid and dashed lines indicate, respectively $y_0 \geq -\beta/\gamma$ (Side = R) and $y_0 < -\beta/\gamma$ (Side = L).

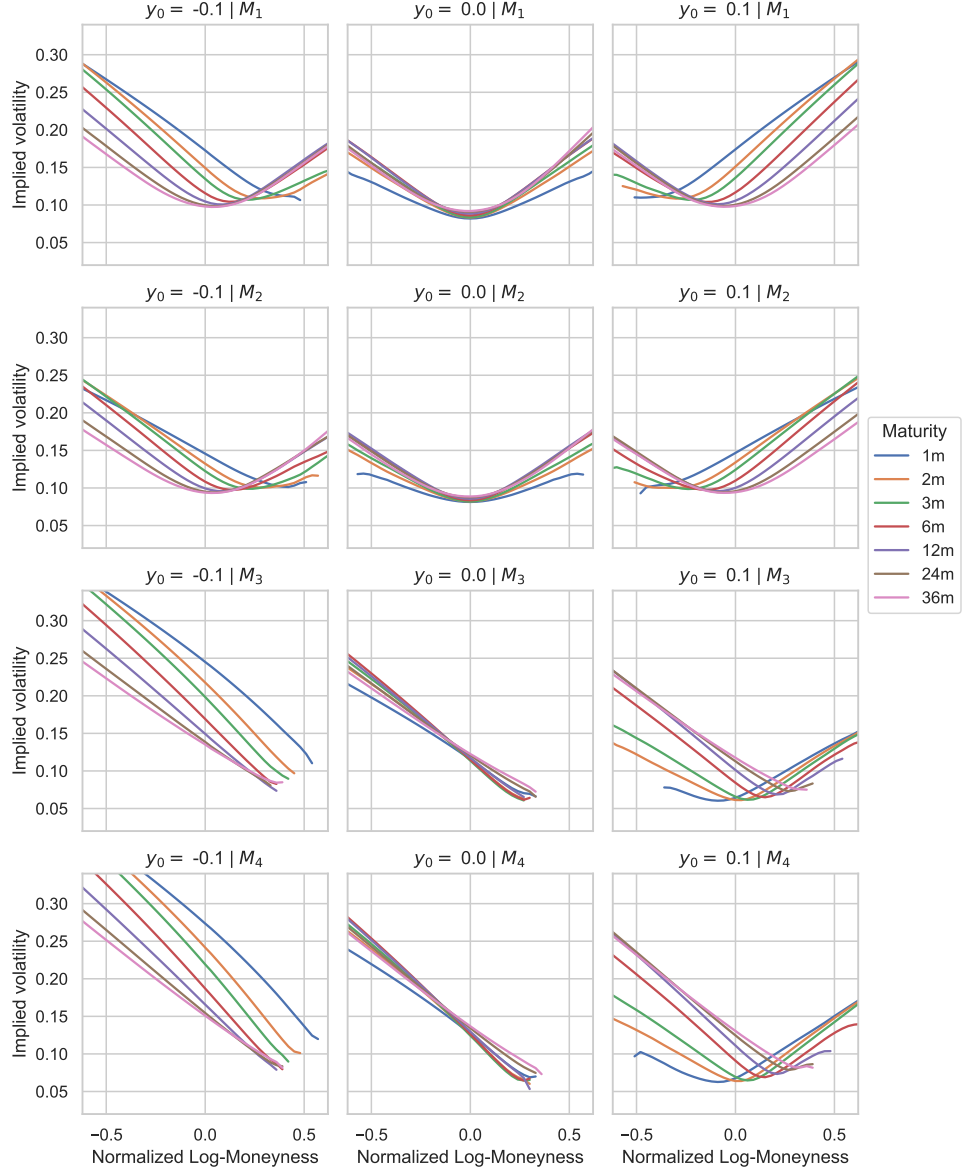


Figure 4: Implied volatility smiles under models $M_1 - M_4$ (rows) in terms of the Log-Moneyness $\log(K) - x_0$ with K is option exercise price. The price of the underlying is $e^{x_0} = 1$ and level of the offset is reported on top of each plot ($y_0 = -.1$ on the left, $y_0 = 0$ at the center and $y_0 = .1$ on the right). Implied volatilities refer to prices computed by means of an Euler-MC method with antithetic variables using 250 time-steps per year and 10^6 trajectories.

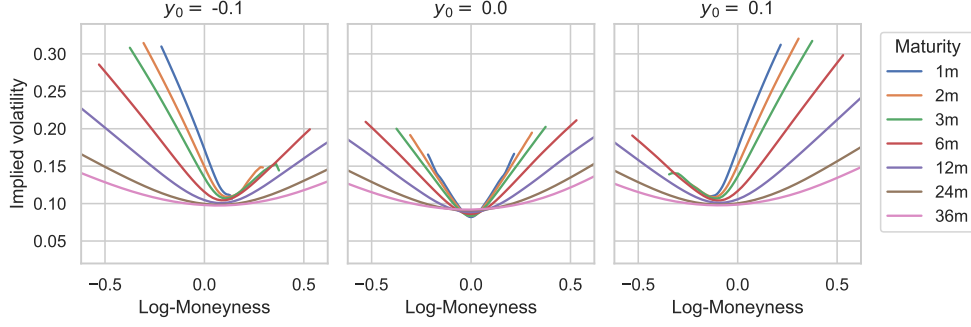


Figure 5: Implied volatility smiles under models $M_1 - M_4$ (rows). The price of the underlying is $e^{x_0} = 1$ and level of the offset is reported on top of each plot. On the x-axis the “Normalised Log-Moneyness” $\log(K)/\sqrt{T}$, with K being the strike price. Option prices computed by an Euler-MC method with antithetic variables using 250 time-steps per year and 10^6 trajectories.

the offset becomes large and positive (here $y_0 = 0.1$) some smile loses its monotonous characteristics. Recall that, for those models, the spot volatility minimum is located at an offset $y_t = 0.06$.

Next, Figure 6 shows on the top the term structure of the ATM implied volatility and its skew. More precisely, if $\sigma_{impl}(\ell, T)$ denotes the implied volatility for log-moneyness $\ell = \log(K/S_0)$ and maturity T , the ATM-Volatility and ATM-Skew term structures are, respectively, the functions

$$\text{ATM-Volatility: } T \rightarrow \sigma_{impl}(0, T) \quad \text{and} \quad \text{ATM-Skew: } T \rightarrow \left. \frac{d\sigma_{impl}(x, T)}{d\ell} \right|_{\ell=0}. \quad (36)$$

In these tests, that derivative is approximated by finite differences. The symmetry of models M_1 and M_2 does not deserve further comments. The following remarks refers to the asymmetric models M_3 and M_4 . Firstly, the ATM volatility qualitatively parallels the forward volatility shapes seen in Figure 3. Next, in neutral ($y_0 = 0$) and “bear” ($y_0 = -0.1$) market states the Skews term structures are both monotonically decreasing and not very different, qualitatively confirming stylised facts observed on market skews. However, when the market had a “bull” trajectory, that decreasing pattern is inverted for short maturities.

3.2. Rank-one QHR model

Consider a QHR model where the variance function depends on a single offset: $\eta_t = \mathbf{w}^T \mathbf{y}_t$ where $\mathbf{w} \in \mathbb{R}_+^p$ is such that $\mathbf{w}^T \mathbf{b} = 1$. In this case, the variance function has the shape given in (12) with $r = 1$ and β_0, γ_0 scalar. This model will be called the Rank-One QHR (R1QHR) model.

As described in the introduction, the offset process \tilde{y}_t can be interpreted as a moving

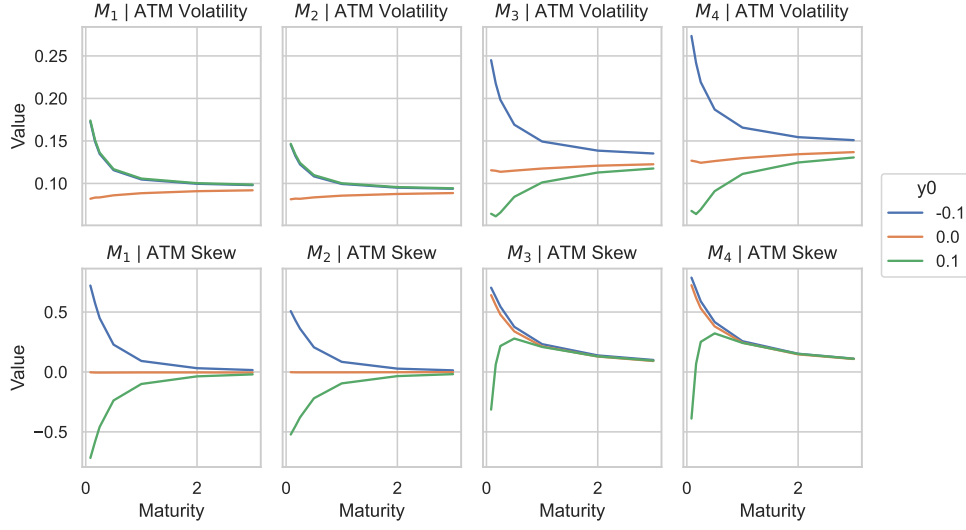


Figure 6: Term structure of ATM-Volatility (top) and ATM-Skew (bottom) as defined in (36).

average using the filter φ defined in (4). That is

$$\tilde{y}_t = \xi_t - \int_{\infty}^t \varphi(t-s) \xi_s ds,$$

because $\mathbf{w}^T \mathbf{b} = 1$. Moreover, the second part of Assumption 1 reduces to the constraints $\alpha > 0$ and $\beta_0^2 \leq \alpha \gamma_0$.

Notice that, although σ_t^2 is function of the scalar process η_t , the dimension of the SDE (6b) cannot be reduced without loosing its Markovian property. Indeed, the dynamics of η , that is

$$d\eta_t = \mathbf{w}^T \mathbf{A} \mathbf{y}_t dt + \sigma_t dW_t,$$

has a trend that does not depend on η_t only.

In the distinct roots and single root special cases the constants κ and $\tilde{\kappa}$ defined in (19) and (20) reduce to

$$\begin{aligned} \text{Distinct Roots:} \quad \kappa &= \gamma_0 \sum_{i,j=1}^p \frac{1}{\lambda_i + \lambda_j} w_i w_j, & \tilde{\kappa} &= \gamma_0 \lambda_{\min} \left(\sum_{i=1}^p \frac{w_i}{\lambda_i} \right)^2, \\ \text{Single Root:} \quad \kappa &= 2 \frac{\gamma_0}{\lambda_1} \sum_{i,j} \binom{i+j-2}{i-1} \frac{w_i}{2^i} \frac{w_j}{2^j} & \tilde{\kappa} &= \frac{\gamma_0}{\lambda_1} \left(\sum_{i=1}^p w_i \right)^2. \end{aligned}$$

In the case of distinct roots with $\mathbf{w} > 0$, the roots of $\tilde{\mathbf{A}}$ of the rank-one model are all reals. Indeed, in that case matrix $\mathbf{A}_{22} = \tilde{\mathbf{A}} - \mathbf{1} \gamma^T$ with $\tilde{\mathbf{A}}$ diagonal and $\gamma \geq 0$. It is not hard to prove that, for that reason, all the eigenvalues of \mathbf{A}_{22} are real (see Proposition 4 in Appendix A).

3.2.1. Numerical Tests

The above R1QHR model is here numerically tested on a set of models with two offset processes ($p = 2$). Table 3 shows the setup used on these five models. The first four models, namely MM_1, \dots, MM_4 , have two distinct roots ($n = 2, m = 1$), while model MM_5 have a single root ($n = 1$) with double multiplicity ($m = 2$). In that table the first six columns reports the parameters used for each model, while the remaining ones some statistics on them. In particular, μ_2, μ_3 and μ_4 are the smallest real part of the eigenvalues of \mathbf{A}_{22} , \mathbf{A}_{33} and \mathbf{A}_{44} , respectively. The successive column shows the value of κ . Note that, even though κ is not always smaller than $1/3$ all the models are stable since μ_2, μ_3 and μ_4 is positive. The column \mathbf{y}_{\min} shows a value for \mathbf{y} that minimises the variance function. Being not strictly convex, the variance minima belong to a line passing through \mathbf{y}_{\min} orthogonal to \mathbf{w} . The successive columns show the minimum value for the spot volatility, and the asymptotic (stationary) volatility and kurtosis.

Table 3: Setups used for the experimental results.

Model	\mathbf{A}	\mathbf{b}	\mathbf{w}	α	β_0	γ_0
MM_1	$\begin{pmatrix} 1 & 0 \\ -1 & 6 \end{pmatrix}$	$\begin{pmatrix} 1 \\ 0 \end{pmatrix}$	$\begin{pmatrix} 0.2 \\ 0.8 \end{pmatrix}$	0.0100	0.0000	2.00
MM_2	$\begin{pmatrix} 1 & 0 \\ -1 & 6 \end{pmatrix}$	$\begin{pmatrix} 1 \\ 0 \end{pmatrix}$	$\begin{pmatrix} 0.2 \\ 0.8 \end{pmatrix}$	0.0100	0.0000	2.80
MM_3	$\begin{pmatrix} 1 & 0 \\ -1 & 6 \end{pmatrix}$	$\begin{pmatrix} 1 \\ 0 \end{pmatrix}$	$\begin{pmatrix} 0.2 \\ 0.8 \end{pmatrix}$	0.0144	-0.1825	2.80
MM_4	$\begin{pmatrix} 1 & 0 \\ -1 & 12 \end{pmatrix}$	$\begin{pmatrix} 1 \\ 0 \end{pmatrix}$	$\begin{pmatrix} 0.2 \\ 0.8 \end{pmatrix}$	0.0144	-0.2365	4.70
MM_5	$\begin{pmatrix} 6 & 0 \\ -1 & 6 \end{pmatrix}$	$\begin{pmatrix} 1 \\ 0 \end{pmatrix}$	$\begin{pmatrix} 1.0 \\ 0.2 \end{pmatrix}$	0.0144	-0.1889	3.00

Model	μ_2	μ_3	μ_4	κ	$\tilde{\kappa}$	\mathbf{y}_{\min}	σ_{\min}	$\sqrt{v_{\infty}}$	Kurt $_{\infty}$
MM_1	1.75	2.28	2.60	0.10	0.49	$\begin{pmatrix} 0.0000 \\ 0.0000 \end{pmatrix}$	10.00%	10.55%	1.03
MM_2	1.66	2.01	2.11	0.14	0.68	$\begin{pmatrix} 0.0000 \\ 0.0000 \end{pmatrix}$	10.00%	10.79%	1.07
MM_3	1.66	2.01	2.11	0.14	0.68	$\begin{pmatrix} 0.0192 \\ 0.0767 \end{pmatrix}$	5.00%	12.95%	1.90
MM_4	1.66	1.98	1.99	0.16	2.26	$\begin{pmatrix} 0.0148 \\ 0.0592 \end{pmatrix}$	5.00%	13.10%	2.17
MM_5	8.62	8.42	5.22	0.26	0.54	$\begin{pmatrix} 0.0606 \\ 0.0121 \end{pmatrix}$	5.00%	13.94%	5.93

The setup is designed along the following lines. The comparison starts with a symmetrical model, namely MM_1 , that satisfies the stability sufficient condition $\kappa < 1$. The model is based on a filter which has two roots. The first one ($\lambda_1 = 1$) allows to intercept medium-term effects and the second one ($\lambda_2 = 6$) to short-term effects. The short-term offset has larger weight ($w_2 = 0.8$ vs $w_1 = 0.2$) and thus the volatility is more sensible to fast movements than to deviations from medium-term trends.

Looking at Table 3, this models does not show heavy tails under the stationary regime ($\text{Kurt}_{\infty} < 3$). In model MM_2 , the variance coefficient γ is chosen to that $\kappa = 1/3$. Nevertheless, the model is still stable, as μ_2, μ_3 and μ_4 are positive. Note that, increase on the convexity of the variance function does not change too much the asymptotic volatility, but it has a large effect on the kurtosis.

Model MM_3 is obtained from MM_2 by increasing the coefficient α and moving the

minimum of the variance function. In that model has the volatility can reach a smaller value (5%) but with a larger asymptotic volatility (14.70%). Note that model MM_3 has a very large asymptotic kurtosis.

Next, the fourth model, MM_4 , is designed with aim to have the same characteristics of model MM_3 but with a larger value for the short memory root: $\lambda_2 = 12$. Indeed, the variance function have the same minimum and similar asymptotic value. Differently from the previous model, the condition $\kappa < 1/3$ is not satisfied neither with equality, nevertheless the Kurtosis has a smaller value than in model MM_3 .

Finally, model MM_5 is analogous to model MM_3 but using a filter with a root $\lambda_1 = 6$ with double multiplicity. There, to have a positive filter that integrates to one, the weights are chosen so that $w_1 = 1$ and $w_2 \in [0, 1]$.

Table 4 reports the filter roots λ_1 and λ_2 (first two columns) and the eigenvalues of \mathbf{A}_{22} for the five model. Notice that, the models with distinct roots have, as expected, real eigenvalues and model MM_5 have two conjugate complex roots. Looking at the last column, that eigenvalue is given by the sum of the two filter roots, that is $\lambda_1 + \lambda_2$, for the distinct root case, and by the double of the root for the double multiplicity case $2\lambda_1$.

Table 4: Eigenvalues of the matrices \mathbf{A} (first two columns) and \mathbf{A}_{22} (last four columns).

Model						
MM_1	1.00	6.00	1.89	6.20	10.91	7.00
MM_2, MM_3	1.00	6.00	1.83	5.79	10.58	7.00
MM_4	1.00	12.00	1.74	11.09	21.47	13.00
MM_5	6.00		7.15	$12.93 - 0.96j$	$12.93 + 0.96j$	12.00

The shape of the filters and of their components is shown in Figure 7 for models MM_3, MM_4 and MM_5 . Those of models MM_1 and MM_2 are not explicitly shown because identical to that of MM_3 . Note that, the filter φ_2 of model MM_3 is negative near the origin, but the whole filter φ is positive, since $w_2 = 0.2 < w_1 = 1$. The qualitative properties of those filters are the following. MM_3 and MM_4 have the similar decay (long-memory) and MM_5 have a faster decay. On the short- and medium-term side, MM_3 and MM_5 have similar weight, while MM_4 poses more weight on the short-term information and less on the medium-term one.

Hereafter, only the performances of models MM_3, MM_4 and MM_5 are considered, since the symmetric models are not too much realistic. Figure 8 shows the term structure of the forward instantaneous variance. The plots in the top row show the curve v^0 and v^{\min} defined in (29) and (30). For model MM_1 , the two curves are not distinguishable because of the symmetry. Note that, since $\lim_{s \rightarrow \infty} v_0(s) = \sigma_\infty^2$ for any $\mathbf{y}_t \in \mathbb{R}^p$, both the curves converges asymptotically to σ_∞^2 . At the scale of the plots, this behaviour is clearly visible for models MM_1 and MM_5 .

Another consequence of the symmetry is that since the forward curve depends only on the three factors y_{1t}^2, y_{2t}^2 and $y_{1t}y_{2t}$, and not directly on y_{1t} and y_{2t} . That is, $\psi^{(\mathbf{y})}(s) = 0$.

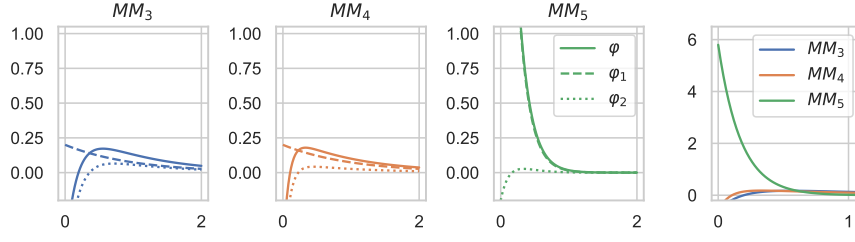


Figure 7: Plot of the filter φ and its components φ_1 and φ_2 for models MM_3 , MM_4 and MM_5 as defined in (4).

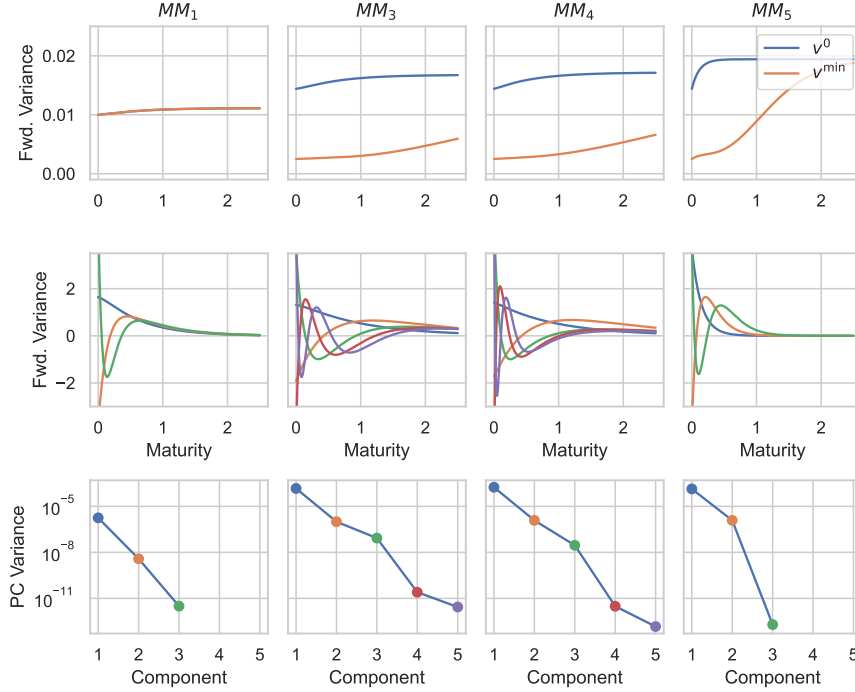


Figure 8: Term structure of instantaneous forward variance. Top: forward variance $v^0 = v_0(\cdot)$ when $y_0 = 0$ and at minimum. Middle: principal components (PC) of the forward variance curve. Bottom: variance of each PC. In the middle and bottom plots, the curve and the variance of each PC is shown using the same color (blue for the first PC, orange for the second one, green for the third one and so on).

As a result, the PCA will have three components with non-null variance as it is shown in the bottom left plots of Figure 8.

Regarding models MM_3 and MM_4 , the first principal component (PC) have a quite fast decay. Then, those with smaller variance have a more slow decay. Indeed, $\lambda_1 = 1$ was chosen with the purpose of introducing a long-memory effect into the model. Next, compare the PCs of model MM_1 and MM_3 , that have the same roots $\lambda_1 = 1$ and $\lambda_2 = 6$, but different asymmetry and convexity. Those differences results on a larger forward curve variance, as seen on the PC variance's plots, and on slower decay of the PCs, as shown by the third (green) and fourth (red) PCs of model MM_3 . On the contrary, all the PCs of MM_5 , the model with a single root of double multiplicity, have a quite fast decay. Also, the variance of the last PCs is quite small (bottom right plot). Moreover, the last two PCs of model MM_3 , having a very small variance, should have a very small effect on the forward variance. Finally note that, the oscillation of the PC curves is an expected consequence of their orthogonality.

Figure 9 shows the implied volatility smiles for the asymmetric models MM_3 , MM_4 and MM_5 for different initial (market) conditions. Recall that for models MM_3 and MM_4 the two elements of the initial condition \mathbf{y}_0 corresponds to offsets w.r.t. "long" term and short term memory averages. The first initial condition $\mathbf{y}_0 = (0.01, 0.05)$ corresponds to a market where, the underlying is only slightly above the long term trend and consistently above w.r.t. the short term one. For instance, the underlying had a recent growth that allowed to return above its long-term average. The second scenario, $\mathbf{y}_0 = (0.05, 0.05)$, corresponds to a "bull" market where the underlying had a substantial growth w.r.t. both the offsets. In the third scenario, $\mathbf{y}_0 = (0, -0.03)$ the underlying performances are not bad w.r.t. a long-term evaluation, but quite bad for an investor who entered the market only recently. In the fourth setup, $\mathbf{y}_0 = (-0.03, 0)$ those two behaviour are inverted. Finally, $\mathbf{y}_0 = (-0.05, -0.05)$ represents a "bear" market contingency where the underlying under-perform w.r.t. both the averages. Regarding model MM_5 , the first offset is an exponential moving average with memory parameter $\lambda = 6$ as in (11a). As discussed in Section 2.3, the second element of \mathbf{y}_t is the offset between the exponential moving average and a longer memory moving average whose weight is more concentrated at a lag of $1/6$ years, that is 2 months. At a different time scale, the shape of these two filters is shown in the left plot of Figure 1, as a blue and yellow curve.

Regarding the smiles shown in Figure 9, the consequences of bear market, $\mathbf{y}_0 = (-0.05, -0.05)$, are an increase in all the volatility smiles (last row). Comparing the different row of Figure 9, it seems that a variation on only one of the two offsets does not have similar substantial consequences across maturity and moneyness. Rather, that the effects of those changes are a different skew or a later shift of the smile curve. For instance, in the mixed market conditions, $\mathbf{y}_0 = (0, -0.03)$ and $\mathbf{y}_0 = (-0.03, 0)$, the smiles of short-term and long-term maturities crosses (see 3rd and 4th rows of Figure 9).

For the same set of R1QHR models and initial conditions, the ATM-Volatility and ATM-Skew term structures defined in (36) are shown in Figure 10. As expected, the larger value of λ_2 in model MM_4 do not influence too much the long term behaviour

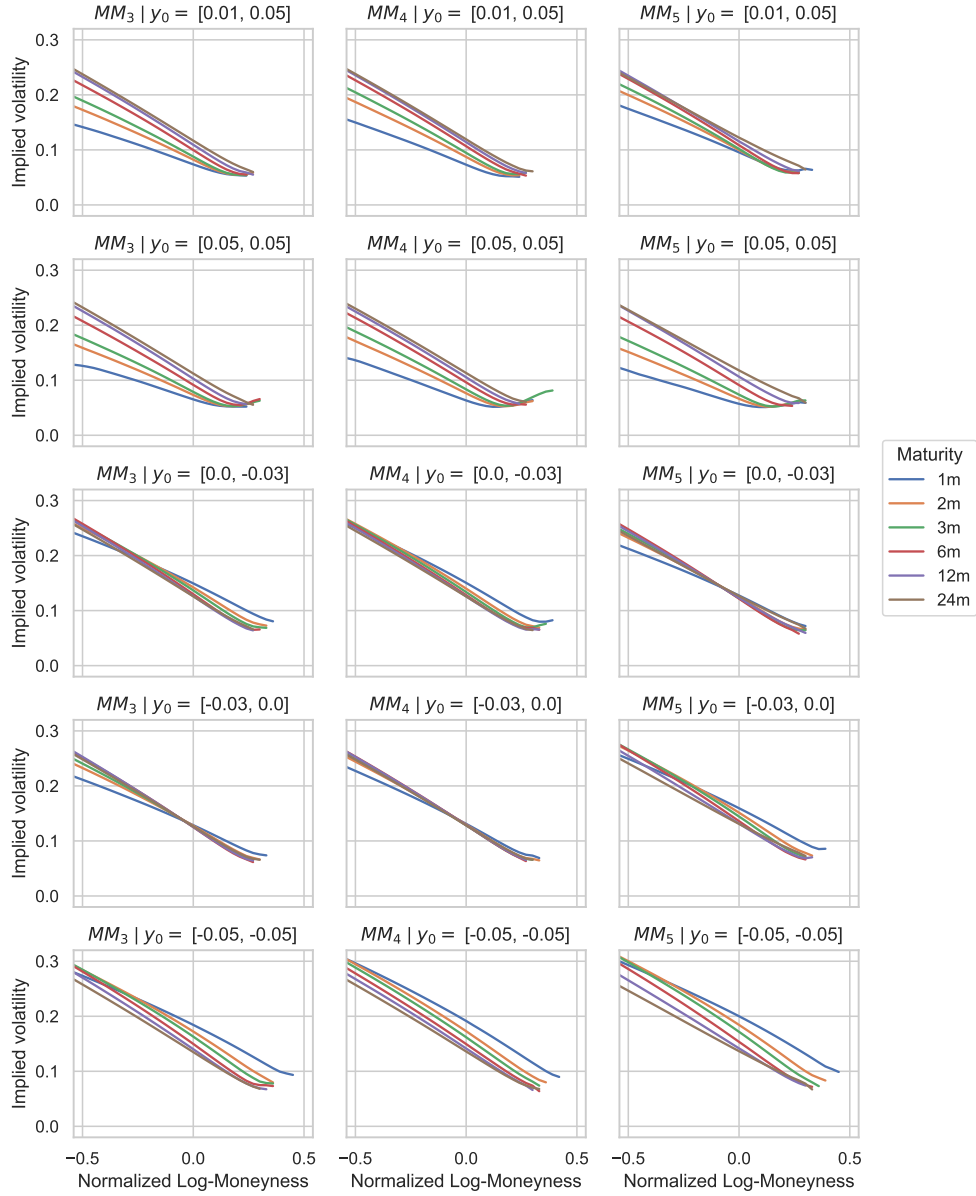


Figure 9: Implied volatility smiles for models MM_3 , MM_4 and MM_5 (columns), different initial conditions y_0 (rows) and maturities T (color). The underlying price is $e^{x_0} = 1$ and the implied volatilities are plotted against the “normalised log-moneyness” $\log(K)/\sqrt{T}$ where K is the strike price. Option prices are computed by means of an Euler-MC method with antithetic variables, 250 time-steps per year and 10^6 trajectories.

of those term structures, but only the short term one. Moreover, the ATM skew term-structure for the model with double multiplicity seems to be quite different from the other two. Qualitatively, the initial condition y_0 affects both the curves homogeneously across models. The only exception is, again, model MM_5 where the ATM curves of the two mixed market conditions (blue and green) are inverted w.r.t. the other two models.

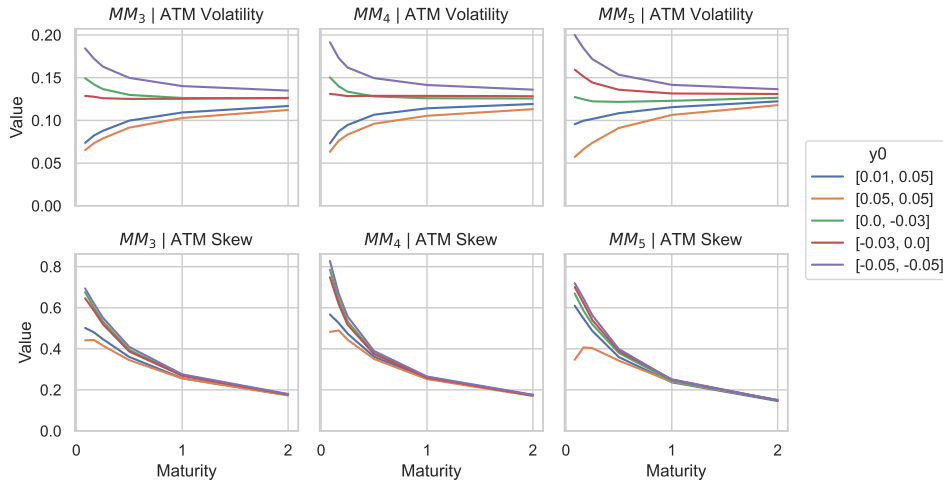


Figure 10: Term structure of ATM Volatility (top) and ATM Skew for models MM_3 , MM_4 and MM_5 .

4. Conclusions and further extensions

This work develop the QHR model, a multifactor quadratic generalisation of the HR model [19] with the following properties:

- Markovianity;
- autonomous and non-dimensional dynamics specification;
- path dependent volatility;
- price and volatility are diffusion processes;
- weak-stationary volatility;
- the variance and the squared increments processes have an ARMA autocorrelation structure;
- allowing for leptos- and platy-Kurtic returns;
- explicit expression for the forward variance;

- flexible forward variance, ATM volatility and ATM skew curves.

The QHR model shares most of those properties with the COGARCH model which requires a driving Levy process with discontinuous paths. Also the quadratic specification for the variance is analogous to quadratic rough-Heston model [13]. Regarding the absence of roughness in QHR volatility model, note that rough models are often approximated by multifactor models analogous to the QHR model [1]. Moreover, to the knowledge of the author, the presence of roughness in financial volatility processes is still debated [7].

Although, the purpose of this paper is to present the model and study the properties of the models, some numerical experiments are reported to show the model capabilities. However, the market performances of the QHR model deserve further research that will consist on the calibration to forward and option prices or on an econometric fitting on historical price trajectories.

Another direction to extend the model here presented is to consider a fully second order model. More precisely, the QHR model is of second order in the sense that the variance is a quadratic function of the first order offset process \mathbf{y}_t . However, a second order model can be also obtained by introducing factor which is a moving average of the squared offsets like the following

$$\mathbf{Z}_t = \int_{-\infty}^t (e^{-\frac{1}{2}\mathbf{A}(t-s)}) \mathbf{y}_s \mathbf{y}_s^T (e^{-\frac{1}{2}\mathbf{A}(t-s)})^T ds.$$

Note that, when $p = 1$, the latter reduces to $z_t = \int_{-\infty}^t e^{-\lambda(t-s)} y_s^2 ds$. Having defined \mathbf{Z}_t , it could be included into the model by defining adding the term $\text{tr}(\mathbf{\Delta Z}_t)$ to the variance specification (6c). Assuming $\mathbf{\Delta} \in \mathcal{S}_+^p$ is sufficient to ensure the positivity of σ_t^2 . It is worth remarking that the original HR setup already considered the use of offsets of some order $m > 1$. However, all the work that originated from it, including the present one, is based on first order offset processes [10, 11, 12, 18, 24].

References

- [1] Eduardo Abi Jaber and Omar El Euch, *Multifactor approximation of rough volatility models*, SIAM J. Financial Math. **10** (2019), no. 2, 309–349. MR 3934104
- [2] O. E. Barndorff-Nielsen, *Superposition of Ornstein-Uhlenbeck type processes*, Teor. Veroyatnost. i Primenen. **45** (2000), no. 2, 289–311. MR 1967758
- [3] Peter Brockwell, Erdenebaatar Chadraa, and Alexander Lindner, *Continuous-time GARCH processes*, Ann. Appl. Probab. **16** (2006), no. 2, 790–826. MR 2244433
- [4] Peter J. Brockwell, *Representations of continuous-time ARMA processes*, J. Appl. Probab. **41A** (2004), 375–382, Stochastic methods and their applications. MR 2057587

- [5] Hans Buehler, *Consistent variance curve models*, Finance and Stoch. **10** (2006), no. 2, 178–203. MR 2223095
- [6] Peter Christoffersen, Kris Jacobs, Chayawat Ornathanalai, and Yintian Wang, *Option valuation with long-run and short-run volatility components*, Journal of Financial Economics **90** (2008), no. 3, 272 – 297.
- [7] Rama Cont and Purba Das, *Rough Volatility: Fact or Artefact?*, Sankhya B **86** (2024), no. 1, 191–223. MR 4733003
- [8] Fulvio Corsi, *A simple approximate long-memory model of realized volatility*, Journal of Financial Econometrics **7** (2009), no. 2, 174–196.
- [9] Giulia Di Nunno, Kęstutis Kubilius, Yuliya Mishura, and Anton Yurchenko-Tytarenko, *From constant to rough: A survey of continuous volatility modeling*, Mathematics **11** (2023), no. 19.
- [10] Gianna Figà-Talamanca and Maria Letizia Guerra, *Fitting prices with a complete model*, Journal of Banking and Finance **30** (2006), no. 1, 247 – 258.
- [11] Paolo Foschi and Andrea Pascucci, *Path Dependent Volatility*, Decis. Econ. Finance **31** (2008), no. 1, 13–32. MR 2385732
- [12] ———, *Calibration of a Path-Dependent Volatility Model: Empirical Taests*, Computational statistics & data analysis **53** (2009), no. 6, 2219–2235, The Fourth Special Issue on Computational Econometrics.
- [13] Jim Gatheral, Paul Jusselin, and Mathieu Rosenbaum, *The quadratic rough Heston model and the joint S&P 500 smile calibration*, Risk (2020).
- [14] Jim Gatheral and Martin Keller-Ressel, *Affine forward variance models*, Finance Stoch. **23** (2019), no. 3, 501–533. MR 3968277
- [15] Guido Gazzani and Julien Guyon, *Pricing and calibration in the 4-factor path-dependent volatility model*, 2024.
- [16] Julien Guyon, *The VIX future in Bergomi models: fast approximation formulas and joint calibration with S&P 500 skew*, SIAM J. Financial Math. **13** (2022), no. 4, 1418–1485. MR 4519245
- [17] Julien Guyon and Jordan Lekeufack, *Volatility is (mostly) path-dependent*, Quant. Finance **23** (2023), no. 9, 1221–1258. MR 4625912
- [18] Vera Blaka Hallulli and Tiziano Vargiolu, *Robustness of the Hobson-Rogers model with respect to the offset function*, Seminar on Stochastic Analysis, Random Fields and Applications V (Basel) (Robert C. Dalang, Francesco Russo, and Marco Dozzi, eds.), Birkhäuser Basel, 2008, pp. 469–492.

- [19] David G. Hobson and L. C. G. Rogers, *Complete models with stochastic volatility*, Math. Finance **8** (1998), no. 1, 27–48. MR 1613366
- [20] Alex Lipton and Adil Reghai, *SPX, VIX and scale-invariant LSV*, 2023, Available at SSRN: <http://dx.doi.org/10.2139/ssrn.4356976>.
- [21] Jan R. Magnus and Heinz Neudecker, *Matrix differential calculus with applications in statistics and econometrics*, Wiley Series in Probability and Statistics, John Wiley & Sons Ltd., Chichester, 1999, Revised reprint of the 1988 original. MR MR1698873 (2000d:15001)
- [22] Karl Pearson, *Contributions to the mathematical theory of evolution. II. Skew variation in homogeneous material*, Phil. Trans. R. Soc. Lond. A **186** (1895).
- [23] Robert J. Plemmons, *M-matrix characterizations. I. Nonsingular M-matrices*, Linear Algebra Appl. **18** (1977), no. 2, 175–188. MR 444681
- [24] Mauro Rosestolato, Tiziano Vargiolu, and Giovanna Villani, *Robustness for path-dependent volatility models*, Decis. Econ. Finance **36** (2013), no. 2, 137–167. MR 3105939
- [25] Eric W. Weisstein, *Pearson system*, From MathWorld—A Wolfram Web Resource.
- [26] Xinyu Zhang and Howell Tong, *Asymptotic theory of principal component analysis for time series data with cautionary comments*, J. Roy. Statist. Soc. Ser. A **185** (2022), no. 2, 543–565. MR 4418430

A. Auxiliary results and proofs

Proposition 4 *Let $\mathbf{D} = \text{diag}(d_1, \dots, d_n)$ and let $\mathbf{x} \in \mathbb{R}_+^n$. Then, all the eigenvalues of $\mathbf{D} - \mathbf{1}\mathbf{x}^T$ are real.*

PROOF Without loss of generality assume that all the zero elements of \mathbf{x} are positioned at the top. Then, \mathbf{x} , \mathbf{D} and $\mathbf{D} - \mathbf{1}\mathbf{x}^T$ can be partitioned as

$$\mathbf{x} = \begin{pmatrix} 0 \\ \mathbf{x}_B \end{pmatrix}, \quad \mathbf{D} = \begin{pmatrix} \mathbf{D}_A & 0 \\ 0 & \mathbf{D}_B \end{pmatrix}, \quad \mathbf{D} - \mathbf{1}\mathbf{x}^T = \begin{pmatrix} \mathbf{D}_A & -\mathbf{1}\mathbf{x}_B^T \\ 0 & \mathbf{D}_B - \mathbf{1}\mathbf{x}_B^T \end{pmatrix},$$

with $\mathbf{x}_B > 0$. We will prove that $\mathbf{M} = \mathbf{D}_B - \mathbf{1}\mathbf{x}_B^T$ is similar to a symmetric matrix. Define $\mathbf{X}_B = \text{diag}(\mathbf{x}_B)$. Then, \mathbf{M} is similar to the matrix $\mathbf{X}_B^{\frac{1}{2}}\mathbf{M}\mathbf{X}_B^{-\frac{1}{2}} = \mathbf{D}_B - \mathbf{X}_B^{\frac{1}{2}}\mathbf{1}\mathbf{1}^T\mathbf{X}_B^{\frac{1}{2}}$, which is symmetric. \blacksquare

PROOF (PROOF OF LEMMA 2) In the following the dynamics of $\mathbf{y}^{\otimes k}$, $2 \leq k \leq 4$, is obtained from (6b) by applying Itô's Lemma. By Lemma 1 also $\mathbf{y}_t^{\otimes k}$ are non-exploding in finite time and also Itô can be safely applied.

- $k = 2$:

Applying Itô to the SDE (6b) and the function $\mathbf{y}_t^{\otimes 2}$ gives

$$\begin{aligned} d\mathbf{y}_t^{\otimes 2} &= (-\mathbf{A}\mathbf{y}_t dt + \mathbf{b}\sigma_t dW_t) \otimes \mathbf{y}_t + \mathbf{y}_t \otimes (-\mathbf{A}\mathbf{y}_t dt + \mathbf{b}\sigma_t dW_t) + (\mathbf{b}\sigma_t) \otimes (\mathbf{b}\sigma_t) dt \\ &= ((\mathbf{b} \otimes \mathbf{b})\sigma_t^2 - (\mathbf{A} \otimes \mathbf{I} + \mathbf{I} \otimes \mathbf{A})\mathbf{y}_t^{\otimes 2}) dt + (\mathbf{b} \otimes \mathbf{y}_t + \mathbf{y}_t \otimes \mathbf{b})\sigma_t dW_t \\ &= (\alpha\bar{\mathbf{b}} + \mathbf{B}^{(2)}(2\beta^T \mathbf{y}_t + \gamma^T \mathbf{y}_t^{\otimes 2}) - \mathbf{A}^{(2)}\mathbf{y}_t^{\otimes 2}) dt + \mathbf{C}^{(2)}\mathbf{y}_t \sigma_t dW_t, \end{aligned}$$

since, from (17), $\mathbf{A}^{(2)} = \mathbf{I}_p \otimes \mathbf{A} + \mathbf{A} \otimes \mathbf{I}_p$, $\mathbf{B}^{(2)} = \bar{\mathbf{b}} = \mathbf{b} \otimes \mathbf{b}$, and $\mathbf{C}^{(2)} = \mathbf{b} \otimes \mathbf{I}_p + \mathbf{I}_p \otimes \mathbf{b}$. Then, using (16),

$$d\mathbf{y}_t^{\otimes 2} = (\alpha\bar{\mathbf{b}} - \mathbf{A}_{12}\mathbf{y}_t - \mathbf{A}_{22}\mathbf{y}_t^{\otimes 2}) dt + \mathbf{C}^{(2)}\mathbf{y}_t \sigma_t dW_t. \quad (37)$$

- $k = 3$.

From (6b) and (37) and applying Itô,

$$\begin{aligned} d\mathbf{y}_t^{\otimes 3} &= d(\mathbf{y}_t \otimes \mathbf{y}_t^{\otimes 2}) \\ &= (\alpha\mathbf{y}_t \otimes \bar{\mathbf{b}} - \mathbf{y}_t \otimes (\mathbf{A}_{12}\mathbf{y}_t) - \mathbf{y}_t \otimes (\mathbf{A}_{22}\mathbf{y}_t^{\otimes 2})) dt \\ &\quad + (\mathbf{y}_t \otimes (\mathbf{C}^{(2)}\mathbf{y}_t))\sigma_t dW_t \\ &\quad - (\mathbf{A}\mathbf{y}_t) \otimes \mathbf{y}_t^{\otimes 2} dt + \mathbf{b} \otimes \mathbf{y}_t^{\otimes 2} \sigma_t dW_t + \mathbf{b} \otimes (\mathbf{C}^{(2)}\mathbf{y}_t)\sigma_t^2 dt \\ &= (\alpha(\mathbf{I}_p \otimes \bar{\mathbf{b}})\mathbf{y}_t - (\mathbf{I}_p \otimes \mathbf{A}_{12})\mathbf{y}_t^{\otimes 3} - (\mathbf{I}_p \otimes \mathbf{A}_{22})\mathbf{y}_t^{\otimes 3} - (\mathbf{A} \otimes \mathbf{I}_p^2)\mathbf{y}_t^{\otimes 3}) dt \\ &\quad + \mathbf{b} \otimes (\mathbf{C}^{(2)}\mathbf{y}_t)\sigma_t^2 dt \\ &\quad + (\mathbf{b} \otimes \mathbf{I}_{p^2})\mathbf{y}_t^{\otimes 2} \sigma_t dW_t + (\mathbf{I}_p \otimes \mathbf{C}^{(2)})\mathbf{y}_t^{\otimes 2} \sigma_t dW_t \\ &= (\alpha(\mathbf{I}_p \otimes \bar{\mathbf{b}})\mathbf{y}_t - (\mathbf{I}_p \otimes \mathbf{A}_{12})\mathbf{y}_t^{\otimes 3} - (\mathbf{I}_p \otimes \mathbf{A}_{22})\mathbf{y}_t^{\otimes 3} - (\mathbf{A} \otimes \mathbf{I}_p^2)\mathbf{y}_t^{\otimes 3}) dt \\ &\quad + (\alpha(\mathbf{b} \otimes \mathbf{C}^{(2)})\mathbf{y}_t + 2(\mathbf{b} \otimes \mathbf{C}^{(2)})\mathbf{y}_t \beta^T \mathbf{y}_t + (\mathbf{b} \otimes \mathbf{C}^{(2)})\mathbf{y}_t \gamma^T \mathbf{y}_t^{\otimes 2}) dt \\ &\quad + \mathbf{C}^{(3)}\mathbf{y}_t^{\otimes 2} \sigma_t dW_t. \end{aligned}$$

In the trend of the latter, the coefficients of \mathbf{y}_t is given by

$$\alpha(\mathbf{I}_p \otimes \bar{\mathbf{b}}) + \alpha(\mathbf{b} \otimes \mathbf{C}^{(2)}) = \alpha \mathbf{B}^{(3)} = -\mathbf{A}_{13},$$

from (16), (17b) and since $\bar{\mathbf{b}} = \mathbf{B}^{(2)}$. Next, the term involving $\mathbf{y}_t^{\otimes 2}$ is given by

$$\begin{aligned} & \left(-(\mathbf{I}_p \otimes \mathbf{A}_{12})\mathbf{y}_t^{\otimes 2} + 2(\mathbf{b} \otimes \mathbf{C}^{(2)})\mathbf{y}_t \beta^T \mathbf{y}_t \right) dt \\ &= 2 \left((\mathbf{I}_p \otimes \mathbf{B}^{(2)} \beta^T) \mathbf{y}_t^{\otimes 2} + (\mathbf{b} \otimes \mathbf{C}^{(2)}) (\mathbf{I}_p \otimes \beta^T) \mathbf{y}_t^{\otimes 2} \right) dt \\ &= 2 \left(\mathbf{I}_p \otimes \mathbf{B}^{(2)} + \mathbf{b} \otimes \mathbf{C}^{(2)} \right) (\mathbf{I}_p \otimes \beta^T) \mathbf{y}_t^{\otimes 2} dt \\ &= 2 \mathbf{B}^{(3)} (\mathbf{I} \otimes \beta^T) \mathbf{y}_t^{\otimes 2} dt \\ &= 2 (\mathbf{B}^{(3)} \otimes \beta^T) \mathbf{y}_t^{\otimes 2} dt = -\mathbf{A}_{23} \mathbf{y}_t^{\otimes 2} dt, \end{aligned}$$

from (16) and (17b). Analogously, the coefficient of $\mathbf{y}_t^{\otimes 3}$ can be rewritten as follows

$$\begin{aligned} & - \left(\mathbf{I}_p \otimes \mathbf{A}_{22} + \mathbf{A} \otimes \mathbf{I}_{p^2} - (\mathbf{b} \otimes \mathbf{C}^{(2)}) \otimes \gamma^T \right) \\ &= -\mathbf{A}^{(3)} + (\mathbf{I}_p \otimes \mathbf{B}^{(2)}) \otimes \gamma^T + (\mathbf{b} \otimes \mathbf{C}^{(2)}) \otimes \gamma^T \\ &= -\mathbf{A}^{(3)} + \mathbf{B}^{(3)} \otimes \gamma^T = -\mathbf{A}_{33}, \end{aligned}$$

since $(\mathbf{b} \otimes \mathbf{C}^{(2)})\mathbf{y}_t \gamma^T \mathbf{y}_t^{\otimes 2} = ((\mathbf{b} \otimes \mathbf{C}^{(2)}) \otimes \gamma^T) \mathbf{y}_t^{\otimes 3}$. Then,

$$d\mathbf{y}_t^{\otimes 3} = - \left(\mathbf{A}_{13} \mathbf{y}_t + \mathbf{A}_{23} \mathbf{y}_t^{\otimes 2} + \mathbf{A}_{33} \mathbf{y}_t^{\otimes 3} \right) dt + \mathbf{C}^{(3)} \mathbf{y}_t^{\otimes 2} \sigma_t dW_t. \quad (38)$$

- $k = 4$.

Analogously to the step $k = 3$, applying Itô's Lemma, rearranging the terms and exploiting the recursions (16) and (17) gives

$$d\mathbf{y}_t^{\otimes 4} = - \left(\mathbf{A}_{24} \mathbf{y}_t^{\otimes 2} + \mathbf{A}_{34} \mathbf{y}_t^{\otimes 3} + \mathbf{A}_{44} \mathbf{y}_t^{\otimes 4} \right) dt + \mathbf{C}^{(4)} \mathbf{y}_t^{\otimes 3} \sigma_t dW_t. \quad (39)$$

Finally, the ODE (14) is obtained from (6b), (37), (38) and (39) by taking the conditional expectations of $\mathbf{y}_t^{\otimes k}$, $1 \leq k \leq 4$. ■

The proof of Lemma 3 reported below will use the following result.

Proposition 5 *If Assumptions 1 and 2 hold, then*

$$\mathbf{A}^{-1} \mathbf{b} > \lambda_{\min}^{-1} \mathbf{b} \geq 0. \quad (40)$$

PROOF Since, $\lambda_{\min} > 0$ by Assumption 1, (40) follows trivially from the structure of \mathbf{A} and \mathbf{b} in Assumption 2 and from the fact that $\mathbf{D}_i^{-1} \mathbf{b}_i = \mathbf{1} \geq \mathbf{b}_i$, $i = 1, \dots, m$. ■

PROOF (PROOF OF LEMMA 3) In the following we will use a vector \mathbf{z} chosen as follows:

$$\mathbf{z} = \mathbf{A}^{-1}\mathbf{b} + \boldsymbol{\xi},$$

where $\boldsymbol{\xi}$ is such that

$$\boldsymbol{\xi} > 0, \quad \mathbf{A}\boldsymbol{\xi} > 0, \quad \boldsymbol{\xi}^T \mathbf{F}\boldsymbol{\xi} + \boldsymbol{\xi}^T \mathbf{F}\mathbf{A}^{-1}\mathbf{b} < \frac{2 - 3\tilde{\kappa}}{3\lambda_{\min}}. \quad (41)$$

Since \mathbf{A} is an M -matrix, it is semi-positive and, thus, there exists a vector satisfying the first two properties in (41). Moreover, since the RHS of the third inequality in (41) is positive, such vector $\boldsymbol{\xi}$ can be rescaled to satisfy all the three inequalities. It follows that \mathbf{z} satisfies the following inequalities

$$\mathbf{A}\mathbf{z} > \mathbf{b}, \quad \mathbf{z} > \mathbf{A}^{-1}\mathbf{b}, \quad \text{and} \quad \boldsymbol{\gamma}^T(\mathbf{z} \otimes \mathbf{z}) < \frac{2}{3\lambda_{\min}}. \quad (42)$$

Moreover, note that under Assumption 2, by Proposition 5,

$$\mathbf{z} > \lambda_{\min}^{-1}\mathbf{b} \geq 0. \quad (43)$$

The proof consists in showing that \mathbf{A}_{22} , \mathbf{A}_{33} and \mathbf{A}_{44} are M -matrices, and, thus, all their eigenvalues have positive real part [23]. Since $\boldsymbol{\gamma} \geq 0$, the matrices \mathbf{A}_{22} , \mathbf{A}_{33} and \mathbf{A}_{44} are Z -matrices. That is, matrices with non-positive off-diagonal elements. To show that those are also M -matrices, it will be shown that they are semi-positive. That is, $\mathbf{A}_{kk}\mathbf{x}_k > 0$ for some $\mathbf{x}_k > 0$ [23]. In particular, that property holds for $\mathbf{x}_k = \mathbf{z}^{\otimes k}$ with $k = 2, 3, 4$.

- $k = 2$. The matrix product $\mathbf{A}_{22}\mathbf{x}_2$ is given by

$$\begin{aligned} \mathbf{A}_{22}\mathbf{x}_2 &= (\mathbf{A} \otimes \mathbf{I} + \mathbf{I} \otimes \mathbf{A} - \bar{\mathbf{b}}\boldsymbol{\gamma}^T)(\mathbf{z} \otimes \mathbf{z}) \\ &> \mathbf{b} \otimes \mathbf{A}^{-1}\mathbf{b} + \mathbf{A}^{-1}\mathbf{b} \otimes \mathbf{b} - \frac{2}{3\lambda_{\min}}\mathbf{b} \otimes \mathbf{b} \quad \text{by (42)} \\ &\geq \frac{4}{3\lambda_{\min}}(\mathbf{b} \otimes \mathbf{b}), \quad \text{by (43)} \end{aligned}$$

and thus $\mathbf{A}_{22}\mathbf{x}_2 > 0$.

- $k = 3$. Firstly note that $\mathbf{B}^{(3)} = \mathbf{b} \otimes \mathbf{b} \otimes \mathbf{I} + \mathbf{b} \otimes \mathbf{I} \otimes \mathbf{b} + \mathbf{I} \otimes \mathbf{b} \otimes \mathbf{b}$ and, thus

$$\begin{aligned} \mathbf{B}^{(3)}(\mathbf{I} \otimes \boldsymbol{\gamma}^T)\mathbf{z}^{\otimes 3} &= \boldsymbol{\gamma}^T(\mathbf{z}^{\otimes 2})(\mathbf{b} \otimes \mathbf{b} \otimes \mathbf{z} + \mathbf{b} \otimes \mathbf{z} \otimes \mathbf{b} + \mathbf{z} \otimes \mathbf{b} \otimes \mathbf{b}) \\ &\leq \frac{2}{3\lambda_{\min}}(\mathbf{b} \otimes \mathbf{b} \otimes \mathbf{z} + \mathbf{b} \otimes \mathbf{z} \otimes \mathbf{b} + \mathbf{z} \otimes \mathbf{b} \otimes \mathbf{b}) \quad \text{by (42)} \\ &\leq \frac{2}{3}(\mathbf{b} \otimes \mathbf{z} \otimes \mathbf{z} + \mathbf{z} \otimes \mathbf{z} \otimes \mathbf{b} + \mathbf{z} \otimes \mathbf{b} \otimes \mathbf{z}) \quad \text{by (43)}. \end{aligned}$$

Moreover,

$$\begin{aligned} \mathbf{A}^{(3)}\mathbf{x}_3 &= (\mathbf{A}\mathbf{z} \otimes \mathbf{z} \otimes \mathbf{z} + \mathbf{z} \otimes \mathbf{A}\mathbf{z} \otimes \mathbf{z} + \mathbf{z} \otimes \mathbf{z} \otimes \mathbf{A}\mathbf{z}) \\ &> (\mathbf{b} \otimes \mathbf{z} \otimes \mathbf{z} + \mathbf{z} \otimes \mathbf{b} \otimes \mathbf{z} + \mathbf{z} \otimes \mathbf{z} \otimes \mathbf{b}). \end{aligned}$$

Thus, $\mathbf{A}_{33}\mathbf{x}_3 > \frac{1}{3}((\mathbf{b} \otimes \mathbf{z} \otimes \mathbf{z} + \mathbf{z} \otimes \mathbf{b} \otimes \mathbf{z} + \mathbf{z} \otimes \mathbf{z} \otimes \mathbf{b})) \geq 0$ and, in turn, \mathbf{A}_{33} is an M -matrix.

- $k = 4$. Finally, to prove that \mathbf{A}_{44} is an M -matrix, note that

$$\begin{aligned}\mathbf{A}^{(4)}\mathbf{x}_4 &= \mathbf{A}\mathbf{z} \otimes \mathbf{z} \otimes \mathbf{z} \otimes \mathbf{z} + \mathbf{z} \otimes \mathbf{A}\mathbf{z} \otimes \mathbf{z} \otimes \mathbf{z} \\ &\quad + \mathbf{z} \otimes \mathbf{z} \otimes \mathbf{A}\mathbf{z} \otimes \mathbf{z} + \mathbf{z} \otimes \mathbf{z} \otimes \mathbf{z} \otimes \mathbf{A}\mathbf{z} \\ &> \mathbf{b} \otimes \mathbf{z} \otimes \mathbf{z} \otimes \mathbf{z} + \mathbf{z} \otimes \mathbf{b} \otimes \mathbf{z} \otimes \mathbf{z} + \mathbf{z} \otimes \mathbf{z} \otimes \mathbf{b} \otimes \mathbf{z} + \mathbf{z} \otimes \mathbf{z} \otimes \mathbf{z} \otimes \mathbf{b}\end{aligned}$$

(by (42))

$$\begin{aligned}\geq \frac{1}{3\lambda_{\min}} &\left(\mathbf{b} \otimes \mathbf{b} \otimes \mathbf{z} \otimes \mathbf{z} + \mathbf{b} \otimes \mathbf{z} \otimes \mathbf{b} \otimes \mathbf{z} + \mathbf{b} \otimes \mathbf{z} \otimes \mathbf{z} \otimes \mathbf{b} \right. \\ &\quad + \mathbf{b} \otimes \mathbf{b} \otimes \mathbf{z} \otimes \mathbf{z} + \mathbf{z} \otimes \mathbf{b} \otimes \mathbf{b} \otimes \mathbf{z} + \mathbf{z} \otimes \mathbf{b} \otimes \mathbf{z} \otimes \mathbf{b} \\ &\quad + \mathbf{b} \otimes \mathbf{z} \otimes \mathbf{b} \otimes \mathbf{z} + \mathbf{z} \otimes \mathbf{b} \otimes \mathbf{b} \otimes \mathbf{z} + \mathbf{z} \otimes \mathbf{z} \otimes \mathbf{b} \otimes \mathbf{b} \\ &\quad \left. + \mathbf{b} \otimes \mathbf{z} \otimes \mathbf{z} \otimes \mathbf{b} + \mathbf{z} \otimes \mathbf{b} \otimes \mathbf{z} \otimes \mathbf{b} + \mathbf{z} \otimes \mathbf{z} \otimes \mathbf{b} \otimes \mathbf{b} \right)\end{aligned}$$

(by (43))

$$\begin{aligned}= \frac{2}{3\lambda_{\min}} &\left(\mathbf{b} \otimes \mathbf{b} \otimes \mathbf{z} \otimes \mathbf{z} + \mathbf{b} \otimes \mathbf{z} \otimes \mathbf{b} \otimes \mathbf{z} + \mathbf{b} \otimes \mathbf{z} \otimes \mathbf{z} \otimes \mathbf{b} \right. \\ &\quad \left. + \mathbf{z} \otimes \mathbf{b} \otimes \mathbf{b} \otimes \mathbf{z} + \mathbf{z} \otimes \mathbf{b} \otimes \mathbf{z} \otimes \mathbf{b} + \mathbf{z} \otimes \mathbf{z} \otimes \mathbf{b} \otimes \mathbf{b} \right).\end{aligned}$$

That is, $\mathbf{A}^{(4)}\mathbf{x}_4 > \frac{2}{3\lambda_{\min}}\mathbf{B}^{(4)}(\mathbf{z} \otimes \mathbf{z})$, and thus

$$\begin{aligned}\mathbf{A}_{44}\mathbf{x}_4 &> \mathbf{B}^{(4)}\left(\frac{2}{3\lambda_{\min}}(\mathbf{z} \otimes \mathbf{z}) - (\mathbf{I}_{p^2} \otimes \boldsymbol{\gamma}^T)(\mathbf{z}^{\otimes 4})\right) \\ &= \mathbf{B}^{(4)}\left(\frac{2}{3\lambda_{\min}}(\mathbf{z} \otimes \mathbf{z}) - \boldsymbol{\gamma}^T(\mathbf{z} \otimes \mathbf{z})(\mathbf{z} \otimes \mathbf{z})\right) \\ &= \mathbf{B}^{(4)}(\mathbf{z} \otimes \mathbf{z})\left(\frac{2}{3\lambda_{\min}} - \boldsymbol{\gamma}^T(\mathbf{z} \otimes \mathbf{z})\right) \geq 0.\end{aligned}$$

Then, since $\mathbf{x}_4 > 0$ and $\mathbf{A}_{44}\mathbf{x}_4 > 0$, \mathbf{A}_{44} is an M -matrix. ■